

**Assessment of liquefaction risk in the Hawke's Bay
Volume 2: Appendices for Volume 1**

BJ Rosser and S Dellow (compilers)

**GNS Science Consultancy Report 2015/186
October 2017**



DISCLAIMER

This report has been prepared by the Institute of Geological and Nuclear Sciences Limited (GNS Science) exclusively for and under contract to Hawke's Bay Regional Council. Unless otherwise agreed in writing by GNS Science, GNS Science accepts no responsibility for any use of or reliance on any contents of this report by any person other than Hawke's Bay Regional Council and shall not be liable to any person other than Hawke's Bay Regional Council, on any ground, for any loss, damage or expense arising from such use or reliance.

Use of Data:

Date that GNS Science can use associated data: October 2017

BIBLIOGRAPHIC REFERENCE

Rosser BJ, Dellow GD, compilers. 2017. Assessment of liquefaction risk in the Hawke's Bay Volume 2: Appendices for Volume 1. Lower Hutt (NZ): GNS Science. 64 p. (GNS Science consultancy report; 2015/186).

AUTHORS

John Begg (GNS Science)
Julia Becker (GNS Science)
Rob Buxton (GNS Science)
Sally Dellow (GNS Science)
Sharn Hainsworth (Landcare Research)
Andrew King (GNS Science)
Virginie Lacrosse (Tonkin & Taylor Ltd.)
Rob Langridge (GNS Science)
Julie Lee (GNS Science)
Sheng-Lin Lin (GNS Science)
Iain Matcham (GNS Science)
Mostafa Nayyerloo (GNS Science)
Zara Rawlinson (GNS Science)
Brenda Rosser (GNS Science)
Wendy Saunders (GNS Science)
Sjoerd van Ballegooij (Tonkin & Taylor Ltd.)

CONTENTS

APPENDICES

A1.0 APPENDIX 1: STEERING GROUP COMMITTEE	1
A2.0 APPENDIX 2: MODIFIED MERCALLI INTENSITY SCALE.....	3
A2.1 REFERENCE.....	6
A3.0 APPENDIX 3: HISTORICAL LIQUEFACTION IN HAWKE'S BAY	7
A3.1 HAWKE'S BAY EARTHQUAKE OF 3 FEBRUARY 1931	7
A3.1.1 Napier (MM10).....	7
A3.1.2 Port Ahuriri; the Westshore causeway, and the Ahuriri lagoon (MM10)	9
A3.1.3 Taradale and the Tutaekuri River (MM10)	9
A3.1.4 Hastings (MM9)	9
A3.1.5 Heretaunga Plains (MM9)	9
A3.1.6 Waiohiki to Puketitiri (MM8–9).....	10
A3.1.7 Poukawa, Te Aute, Otane, Waipawa, and Waipukurau (MM7–8)	11
A3.1.8 Westshore to Mohaka (MM8)	11
A3.1.9 Wairoa (MM8).....	11
A3.2 WAIROA EARTHQUAKE OF 16 SEPTEMBER 1932	11
A3.3 REFERENCES.....	14
A4.0 GEOLOGICAL AND GEOMORPHOLOGICAL MAPPING DATA	15
A4.1 GEOLOGICAL SETTING	15
A4.2 TERRAIN MODELS	18
A4.3 SOILS AND GEOMORPHOLOGY.....	19
A4.3.1 Soil Map Compilation	19
A4.3.2 Geomorphology Map.....	23
A4.4 BOREHOLE DATA.....	25
A4.4.1 Distribution.....	25
A4.4.2 Method of Processing.....	25
A4.4.3 Lithological Data from The Borehole Database	27
A4.4.4 Mapping Dominant Lithology in Boreholes.....	30
A4.4.5 Summary of Borehole Data	31
A4.5 REFERENCES.....	32
A5.0 APPENDIX 5: GEOTECHNICAL DATA, CONE PENETROMETER ANALYSIS, LIQUEFACTION SEVERITY NUMBER AND LAND DAMAGE CORRELATIONS ...	35
A5.1 GEOTECHNICAL DATA.....	35
A5.1.1 Development of A Geotechnical Database for Hawke's Bay	35
A5.2 CPT ANALYSIS.....	35
A5.3 LAND AND BUILDING DAMAGE CORRELATION WITH LSN	38
A5.4 ACRONYMS	44
A5.5 REFERENCES.....	45

A6.0 APPENDIX 6: GROUNDWATER SURFACE MODELLING.....	47
A6.1 WATER LEVEL DATA	48
A6.2 INTERPOLATION METHOD.....	51
A6.3 UNCERTAINTY	56
A6.4 DISCUSSION....	60
A6.5 REFERENCES.....	60
A7.0 APPENDIX 7: TYPICAL LIQUEFACTION DAMAGE	61

APPENDIX FIGURES

Figure A3.1	Isoseismals of the 1931 Hawke's Bay earthquake	8
Figure A3.2	Locations of place names used in this Appendix.....	13
Figure A4.1	Generalised geological map of the Heretaunga Plains, divided into undifferentiated units older than Miocene, Miocene, Pliocene, Quaternary and Holocene.....	17
Figure A4.2	Soil Group.	20
Figure A4.3	Soil Age	21
Figure A4.4	Soil drainage class.	22
Figure A4.5	A generalised geomorphic landforms map of the Heretaunga Plains area.....	24
Figure A4.6	The HBRC boreholes have been clipped to the area of the Heretaunga Plains and are well distributed across the Heretaunga Plains.....	26
Figure A4.7	A Leapfrog cross section from Haumoana to Bluff Hill in the north.	27
Figure A4.8	A map view of the surface and subsurface distribution of Holocene gravels identified from the boreholes.....	28
Figure A4.9	A cross section from Haumoana to Bluff Hill shows some of the Holocene gravel units identified using borehole data.....	28
Figure A4.10	The distribution of shells (green dots) from borehole data that lie above the base of the Holocene surface, showing the maximum inland extent of sea level 7000 years ago.....	29
Figure A4.11	Distribution of the thinned boreholes dataset summarised for predominant lithologies at metre by metre intervals down to 10 m depth, and from 10 to 15m.....	30
Figure A5.1	Map showing the inferred levels of earthquake shaking and the observed land damage for urban residential properties in Christchurch after the (a) 4 September 2010, (b) 22 February 2011, (c) 13 June 2011 and (d) 23 December 2011 earthquakes.	39
Figure A5.2	(a) Box and whisker plot showing the distribution of land damage observations correlated against LSN for the 4 September 2010, 22 February 2011 and 13 June 2011 earthquake events (b) histogram showing the distribution of land damage observations correlated against LSN....	39
Figure A5.3	Frequency bar chart showing the likelihood of none-to-minor, minor-to-moderate, and moderate-to-severe land damage for different LSN bands.....	40
Figure A5.4	(a) Estimated differential foundation settlement from visual inspections of the urban residential buildings in Christchurch as a result of the CES and (b) the associated BDR.....	41
Figure A5.5	(a) Box and whisker plot showing the distribution of differential foundation settlement for residential dwellings in the TC3 and residential Red Zone areas correlated against LSN for the September 2010, February 2011 and June 2011 earthquake events (b) histogram showing the distribution of differential foundation settlement correlated against LSN.	42

Figure A5.6	(a) Box and whisker plot showing the distribution of BDR for the residential dwellings in the TC3 and residential Red Zone areas correlated against LSN for the September 2010, February 2011 and June 2011 earthquake events (b) histogram showing the distribution of BDR correlated against LSN.....	42
Figure A5.7	Frequency bar chart showing the likelihood of differential foundation settlement of less than and greater than 50mm for different LSN bands.	43
Figure A5.8	Frequency bar chart showing the likelihood of BDR values of less than 0.3, 0.3 to 0.5 and greater than 0.5 for different LSN bands.	44
Figure A6.1	Three zones used for developing the unconfined groundwater surface.	47
Figure A6.2	Monitoring well no. 1003.....	48
Figure A6.3	All data used to develop the unconfined groundwater surface.	50
Figure A6.4	Unconfined groundwater surface for Zone 1.	51
Figure A6.5	Unconfined groundwater surface for the northern portion of Zone 2.	52
Figure A6.6	Unconfined groundwater surface for the southern portion of Zone 2.....	53
Figure A6.7	Unconfined groundwater surface for the northern portion of Zone 3.	54
Figure A6.8	Unconfined groundwater surface for the southern portion of Zone 3.....	55
Figure A6.9	Uncertainty map for Zone 1, Wairoa, based on data point density as described in the text.	56
Figure A6.10	Uncertainty map for Zone 2, the Heretaunga Plains, based on data point density as described in the text.....	57
Figure A6.11	Uncertainty map for the northern portion of Zone 3, based on data point density as described in the text.....	58
Figure A6.12	Uncertainty map for the southern portion of Zone 3, based on data point density as described in the text.....	59

APPENDIX TABLES

Table A2.1	Modified Mercalli Intensity scale – NZ 2008 (Dowrick et al, 2008)	3
Table A2.2	Notes to 2007 NZ MM Scale	5
Table A3.1	Observations of liquefaction effects reported in the Hawke's Bay region during historical earthquakes.....	12
Table A5.1	Proxy SV1D and LSN values for various distances from the top of the river bank for main stem channels	36
Table A5.2	Proxy SV1D and LSN values for various distances from the top of the river bank for tributary channels and the lower (downstream) reaches of main-stem channels	37

A1.0 APPENDIX 1: STEERING GROUP COMMITTEE

A technical steering group set up to oversee the project consisted of the following members:

- Brenda Rosser, GNS Science (Project manager)
- Lisa Pearse, HBCDEM (Council Liaison)
- Kelvin Berryman, Natural Hazards Research Platform
- Richard Smith, EQC
- Mike Adye, Hawke's Bay Regional Council
- Bill McWatt, Works Asset Manager, Napier City Council
- Johan Ehlers, Works Asset Development Manager, Napier City Council
- James Minehan, Planner Policy/Analyst, Napier City Council (from August 2015)
- Gerard Van Veen, Building Consents Projects Officer, Hastings District Council
- Murray Arnold, Team Leader Environmental Consents/Subdivision, Hastings District Council
- Malcolm Hart, Community Safety Manager, Hastings District Council
- Peter Eastwood, Central Hawke's Bay District Council
- Charlotte Knight, Wairoa District Council

A2.0 APPENDIX 2: MODIFIED MERCALLI INTENSITY SCALE

Table A2.1 Modified Mercalli Intensity scale – NZ 2008 (Dowrick et al, 2008)

Modified Mercalli Intensity (MM)	People	Fittings	Structures	Environment
MM3	Felt indoors; hanging objects may swing, vibration similar to passing of light trucks, duration may be estimated, may not be recognised as an earthquake.	Generally noticed indoors but not outside. Light sleepers may be awakened. Vibration may be likened to the passing of heavy traffic, or to the jolt of a heavy object falling or striking the building.	Nil	Nil
MM4	Liquids in large open containers may be disturbed (sometimes considerably) in large magnitude (long duration) earthquakes. Pendulum clocks may stop, start, or change rate (H*).	Doors and windows rattle. Glassware and crockery rattle. Liquids in open vessels may be slightly disturbed in small to medium-sized earthquakes. Standing motorcars may rock.	Walls and frames of buildings, and partitions and suspended ceilings in commercial buildings, may be heard to creak.	Nil
MM5	Generally, felt outside and by almost everyone indoors. Most sleepers awakened. A few people alarmed	Small unstable objects are displaced or upset. Some glassware and crockery may be broken. Hanging pictures knock against the wall. Open doors may swing. Cupboard doors secured by magnetic catches may open.	Some Windows Type I* cracked. A few earthenware toilet fixtures cracked, in timber buildings with inadequately braced piles.	Loose boulders may occasionally be dislodged from steep slopes.
MM6	Felt by all. People and animals alarmed. Many run outside. * Difficulty experienced in walking steadily.	Objects fall from shelves. Pictures fall from walls (H*). Some furniture moved on smooth floors, some unsecured free-standing fireplaces moved. Glassware and crockery broken. Very unstable furniture overturned. Small church and school bells ring (H*). Appliances move on bench or table tops. Filing cabinets or 'easy glide' drawers may open (or shut).	Slight damage to Buildings Type I*. Some stucco or cement plaster falls. Windows Type I* broken. Damage to a few weak domestic chimneys, some may fall.	Trees and bushes shake, or are heard to rustle. Loose material may be dislodged from sloping ground, e.g., existing slides, talus and scree slopes. A few very small ($\leq 10^3 \text{ m}^3$) soil and regolith slides and rock falls from steep banks and cuts. A few minor cases of liquefaction (sand boil) in highly susceptible alluvial and estuarine deposits.
MM7	General alarm. Difficulty experienced in standing. Noticed by motorcar drivers who may stop.	Large bells ring. Furniture moves on smooth floors, may move on carpeted floors. Substantial damage to fragile* contents of buildings.	Unreinforced stone and brick walls cracked. Buildings Type I cracked some with minor masonry falls. A few instances of damage to Buildings Type II. Unbraced parapets, unbraced brick gables, and architectural ornaments fall. Roofing tiles, especially ridge tiles may be dislodged. Many unreinforced domestic chimneys damaged, often falling from roof-line. Water tanks Type I* burst. A few instances of damage to brick veneers and plaster or cement-based linings. Unrestrained water cylinders (Water Tanks Type II*) may move and leak. Some Windows Type II* cracked. Suspended ceilings damaged.	Water made turbid by stirred up mud. Small slides such as falls of sand and gravel banks, and small rock-falls from steep slopes and cuttings common. Instances of settlement of unconsolidated, or wet, or weak soils. A few instances of liquefaction (i.e., small water and sand ejections). Very small ($\leq 10^3 \text{ m}^3$) disrupted soil slides and falls of sand and gravel banks, and small rock falls from steep slopes and cuttings are common. Fine cracking on some slopes and ridge crests. A few small to moderate landslides ($10^3 - 10^5 \text{ m}^3$), mainly rock falls on steeper slopes ($>30^\circ$) such as gorges, coastal cliffs, road cuts and excavations. Small discontinuous areas of minor shallow sliding and mobilisation of scree slopes in places. Minor to widespread small failures in road cuts in more susceptible materials. A few instances of non-damaging liquefaction (small water and sand ejections) in alluvium.
MM8	Alarm may approach panic. Steering of motorcars greatly affected.	Same as above as threshold reached at a lower level of shaking	Building Type I, heavily damaged, some collapse*. Buildings Type II damaged, some with partial collapse*. Buildings Type III damaged in some cases*. A few instances of damage to Structures Type IV. Monuments and	Cracks appear on steep slopes and in wet ground. Significant landsliding likely in susceptible areas. Small to moderate ($10^3 - 10^5 \text{ m}^3$) slides widespread; many rock and disrupted soil falls on steeper slopes (steep banks, terrace edges, gorges, cliffs, cuts etc.). Significant areas of shallow regolith landsliding, and some reactivation of scree slopes. A few large ($10^5 - 10^6 \text{ m}^3$) landslides from coastal cliffs, and possibly large to very large ($\geq 10^6 \text{ m}^3$) rock slides and avalanches from

Modified Mercalli Intensity (MM)	People	Fittings	Structures	Environment
			pre-1976 elevated tanks and factory stacks twisted or brought down. Some pre-1965 infill masonry panels damaged. A few post-1980 brick veneers damaged. Decayed timber piles of houses damaged. Houses not secured to foundations may move, and damage to earthenware sanitary fittings may occur. Most unreinforced domestic chimneys damaged, some below roof-line, many brought down.	steep mountain slopes. Larger landslides in narrow valleys may form small temporary landslide-dammed lakes. Roads damaged and blocked by small to moderate failures of cuts and slumping of road-edge fills. Evidence of soil liquefaction common, with small sand boils and water ejections in alluvium, and localised lateral spreading (fissuring, sand and water ejections) and settlements along banks of rivers, lakes, and canals etc. Increased instances of settlement of unconsolidated, or wet, or weak soils.
MM9	Same as above as threshold reached at a lower level of shaking	Same as above as threshold reached at a lower level of shaking	Many Buildings Type I destroyed*. Buildings Type II heavily damaged, some collapse*. Buildings Type III damaged, some with partial collapse*. Structures Type IV damaged in some cases, some with flexible frames seriously damaged*. Damage or permanent distortion to some Structures Type V*. Houses not secured to foundations shifted off. Brick veneers fall and expose frames.	Cracking of ground conspicuous. Landsliding widespread and damaging in susceptible terrain, particularly on slopes steeper than 20°. Extensive areas of shallow regolith failures and many rock falls and disrupted rock and soil slides on moderate and steep slopes (20°–35° or greater), cliffs, escarpments, gorges, and man-made cuts. Many small to large (10^3 – 10^6 m 3) failures of regolith and bedrock, and some very large landslides (10^6 m 3 or greater) on steep susceptible slopes. Very large failures on coastal cliffs and low-angle bedding planes in Tertiary rocks. Large rock/debris avalanches on steep mountain slopes in well-jointed greywacke and granitic rocks. Landslide-dammed lakes formed by large landslides in narrow valleys. Damage to road and rail infrastructure widespread with moderate to large failures of road cuts and slumping of road-edge fills. Small to large cut slope failures and rock falls in open mines and quarries. Liquefaction effects widespread with numerous sand boils and water ejections on alluvial plains, and extensive, potentially damaging lateral spreading (fissuring and sand ejections) along banks of rivers, lakes, canals etc.). Spreading and settlements of river stop-banks likely.
MM10	Same as above as threshold reached at a lower level of shaking	Same as above as threshold reached at a lower level of shaking	Most Buildings Type I destroyed*. Many Buildings Type II destroyed*. Buildings Type III heavily damaged, some collapse*. Structures Type IV damaged, some with partial collapse*. Structures Type V moderately damaged, but few partial collapses. A few instances of damage to Structures Type VI. Some well-built* timber buildings moderately damaged (excluding damage from falling chimneys).	Landsliding very widespread in susceptible terrain. Similar effects to MM9, but more intensive and severe, with very large rock masses displaced on steep mountain slopes and coastal cliffs. Landslide-dammed lakes formed. Many moderate to large failures of road and rail cuts and slumping of road-edge fills and embankments may cause great damage and closure of roads and railway lines. Liquefaction effects (as for MM9) widespread and severe. Lateral spreading and slumping may cause rents over large areas, causing extensive damage, particularly along river banks, and affecting bridges, wharfs, port facilities, and road and rail embankments on swampy, alluvial or estuarine areas.
MM11	Same as above as threshold reached at a lower level of shaking	Same as above as threshold reached at a lower level of shaking	Most Buildings Type II destroyed *. Many Buildings Type III destroyed *. Structures Type IV heavily damaged, some collapse*. Structures Type V damaged, some with partial collapse. Structures Type VI suffer minor damage, a few moderately damaged.	Environmental response criteria have not been suggested for MM11 as that level of shaking has not been reported in New Zealand or (definitively) elsewhere.

Items marked * in the scale are defined in the notes following.

Table A2.2 Notes to 2007 NZ MM Scale

	Construction types	NZ 1966 MM scale equivalent	Definition
Buildings	Type I	Masonry D	Buildings with low standard of workmanship, poor mortar, or constructed of weak materials like mud brick or rammed earth soft storey Structures (e.g., shops) made of masonry, weak reinforced concrete or composite materials (e.g., some walls timber, some brick) not well tied together. Masonry buildings otherwise conforming to buildings Types I–III, but also having heavy unreinforced masonry towers. (Buildings constructed entirely of timber must be of extremely low quality to be Type I).
	Type II	Masonry C	Buildings of ordinary workmanship, with mortar of average quality. No extreme weakness, such as inadequate bonding of the corners, but neither designed nor reinforced to resist lateral forces. Such buildings not having heavy unreinforced masonry towers.
	Type III	Masonry B	Reinforced masonry or concrete buildings of good workmanship and with sound mortar, but not formally designed to resist earthquake forces.
Structures	Type IV	Masonry A	Buildings and bridges designed and built to resist earthquakes to normal use standards, i.e., no special collapse or damage limiting measures taken (mid-1930's to c. 1970 for concrete and to c. 1980 for other materials).
	Type V		Buildings and bridges, designed and built to normal use standards, i.e., no special damage limiting measures taken, other than code requirements, dating from since c. 1970 for concrete and c. 1980 for other materials.
	Type VI		Structures, dating from c. 1980, with well-defined foundation behaviour, which have been specially designed for minimal damage, e.g., seismically isolated emergency facilities, some structures with dangerous or high contents, critical facilities which must remain operational after earthquakes, or new generation low damage structures.
Windows	Type I		Large display windows, especially shop windows.
	Type II		Ordinary sash or casement windows.
	Water Tanks		
	Type I		External, stand mounted corrugated iron tanks.
	Type II		Domestic hot-water cylinders unrestrained except by supply and delivery pipes.
	H		(Historical) More likely to be used for historical events.

Other Comments

“Some” or “a few” indicates that the threshold of a particular effect has just been reached at that intensity.

“Many run outside” (MM6) variable depending on mass behaviour, or conditioning by occurrence or absence of previous quakes, i.e., may occur at MM5 or not till MM7.

“Fragile Contents of Buildings”: Fragile contents include weak, brittle, unstable, unrestrained objects in any kind of building.

“Well-built timber buildings” have: wall openings not too large; robust piles or reinforced concrete strip foundations; superstructure tied to foundation.

Buildings Type III–V at MM10 and greater intensities are more likely to exhibit the damage levels indicated for low-rise buildings on firm or stiff ground and for high-rise buildings on soft ground. By inference, lesser damage to low-rise buildings on soft ground and high-rise buildings on firm or stiff ground may indicate the same intensity. These effects are due to attenuation of short period vibrations and amplification of longer period vibrations in soft soils.

A2.1 REFERENCE

Dowrick DJ, Hancox GT, Perrin ND, Dellow GD. 2008 The Modified Mercalli intensity scale: revisions arising from New Zealand experience. *Bulletin of the New Zealand Society for Earthquake Engineering*, 41(3): 193-205.

A3.0 APPENDIX 3: HISTORICAL LIQUEFACTION IN HAWKE'S BAY

Dellow et al. (1999) compiled information on earthquakes which caused significant damage within Hawke's Bay (MM7 or greater, Table A3.1) and described the accompanying areas of liquefaction and/or minor disruption of services. Sources of information include unpublished isoseismal maps (Dowrick), published papers by Downes (1995) and Hancox et al. (1997, 2002), other unpublished data (Downes & Dowrick) and reports held on GNS files. The Hawke's Bay Earthquake of 3 February 1931 and the Wairoa Earthquake of 16 September 1932 are the two historic earthquakes that have caused the greatest shaking intensities and liquefaction damage in the Hawke's Bay region, and are examples of the distribution and severity of liquefaction that can be expected in future large earthquakes. The distribution and impacts from liquefaction in these two earthquakes are summarised below. The reader is referred to Dellow et al. (1999) for descriptions of liquefaction effects from other historic earthquakes listed in Table A3.1.

A3.1 HAWKE'S BAY EARTHQUAKE OF 3 FEBRUARY 1931

The 1931 Hawke's Bay earthquake caused the greatest loss of life and the most extensive damage ever recorded for an earthquake in New Zealand (Callaghan 1933). As shown in Figure A3.1 (from Dowrick 1998) the effects of the earthquake were greatest in the towns of Napier (MM10) and Hastings (MM9), but other towns in the Hawke's Bay region also suffered major damage – Havelock North MM9; Waipawa, Waipukurau, Te Aute, Wairoa MM8; Gisborne MM7. The official death toll was 256, 161 occurring in Napier, 93 in Hastings and 2 in Wairoa (McSaveney 2017). The earthquake was followed by fires in the central business areas of both Napier and Hastings. The fires raged uncontrollably in Napier as the water supply for firefighting was cut-off because of the many broken water mains. However, in Hastings an uninterrupted water supply was available thus enabling the fires to be brought under control much more effectively (Butcher 1931).

The earthquake epicentre was located 30 km to the NNE of Napier, and the magnitude is estimated at $M_s = 7.8$ (Dowrick & Smith 1990). The earthquake was felt throughout most of New Zealand and was accompanied by well-documented faulting and uplift, with extensive liquefaction and related fissuring and slumping, and landslides occurring over much of Hawke's Bay (Henderson 1933; Hull 1990). These effects resulted in widespread disruption to services, road and rail traffic. There was permanent change in local drainage patterns as seen by the shift in the mouth of the Tutaekuri River. Ground subsidence of alluvial materials was widespread, and liquefaction (sand boils) apparently occurred over a wide area, including Wairoa, Mohaka, Tongioio, Petane, Napier, Taradale and the Heretaunga Plains (Fairless & Berrill 1984). The liquefaction effects in different locations in Hawke's Bay are described below. Modified Mercalli (MM) shaking intensities assigned to these locations are as assigned by Dowrick (1998), see Figure A3.1.

A3.1.1 Napier (MM10)

The epicentre of the magnitude 7.8 earthquake was located close to Napier and caused MM10 intensity shaking in the Napier area. Analysis of the distribution of damage from this event indicates that the greatest damage occurred on soils formed on reclaimed swamp and lagoon areas that suffered from liquefaction effects (Dowrick 1998). In the Port Ahuriri and Napier South areas, differential settlement of buildings occurred that were founded on silt. In Napier, the water-supply was seriously interrupted by the earthquake, cast-iron mains were badly fractured at junctions, and at joints, the lead packings were disturbed, allowing extensive leakage (Brodie & Harris 1933). The sewerage system was also badly damaged. Damage to buried services was

greater in Napier South, on land reclaimed from the former Ahuriri lagoon, where ground fissures were much more evident (Conly 1931; Butcher 1931). Cracks and fissures appeared on the streets of Napier and were most pronounced along the original bed of the former Tutaekuri River (Callaghan 1933). In places where the Tutaekuri River had been diverted, the surface of the former channel sank by as much as 1m (near the boys' college), allowing the old course of the Tutaekuri River to be readily traced through Napier (Henderson 1933).

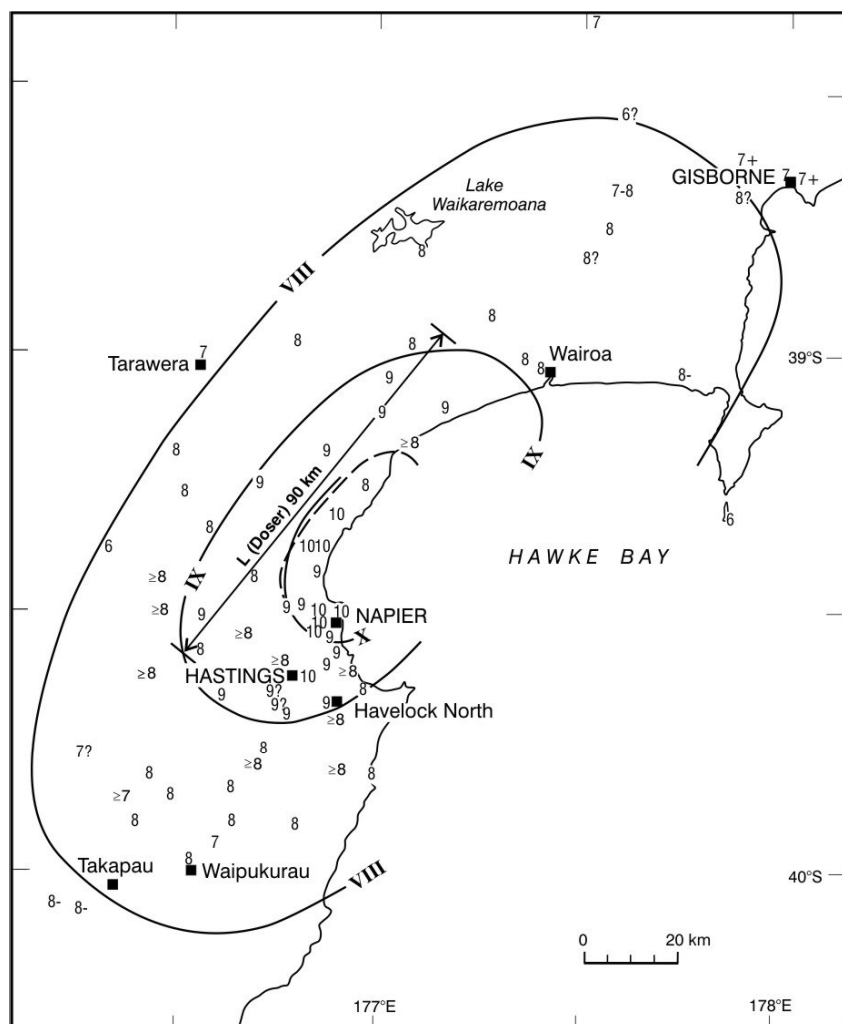


Figure A3.1 Isoseismals of the 1931 Hawke's Bay earthquake (from Dowrick, 1998).

The damage descriptions given above reveal that liquefaction occurred within the young (Holocene), weak, fine-grained lagoonal sediments in and around Napier. Areas where fill had been placed on these sediments were also affected with the loose fill and/or sediments (including peat) consolidating during the earthquake shaking. No mention was made in these descriptions of water and sand being ejected associated with the fissuring and this may indicate that the process was more akin to lateral spreading, albeit incipient, as there is also no mention of large displacements.

A3.1.2 Port Ahuriri; the Westshore causeway, and the Ahuriri lagoon (MM10)

Severe liquefaction occurred on the area of reclaimed land between Scinde Island and the original eastern spit (Port Ahuriri) and the Ahuriri lagoon, with lateral spreading occurring along the margins of the main tidal channels in the lagoon. Differential settlements were common, especially in areas where fill had been placed, and produced extensive fissuring. The extensive fills in this area were badly affected, primarily because of the weak nature of the foundation materials. Sand boils were reported at only one site, which may be a reflection of the finer grained nature of the natural sediments which are invariably referred to as mud (silts and clays). The primary mode of failure in such fine-grained material appears to be differential settlement which resulted in the occurrence of fissures, the density of the fissuring being a function of the intensity of the ground shaking and the strength (generally weak to very weak) of these soils.

A3.1.3 Taradale and the Tutaekuri River (MM10)

In the area between the Tutaekuri River, the former Ahuriri lagoon and the low hills to the east and north of Taradale, Henderson (1933) reported abundant fissuring, lateral spreads and settlements. Fissures opened at many points along the river channels, especially where these crossed the Heretaunga Flats, and were particularly noticeable along the Tutaekuri River near Napier where roads were split, water and sewer pipes ruptured, and houses displaced. In some places, the ground moved toward the channel by as much as 3m. No reference was found to indicate that sand and water were ejected from these fissures. This may indicate that the strength of the ground shaking was such that lateral spreading occurred and that this represents the behaviour of these materials at a shaking intensity of MM10. It is interesting to note that at MM7 (1863, 1904) sand boils were observed in this area (Table A3.1), and that at MM10 (1931) extensive lateral spreading occurred. Unfortunately, there are no historical events which have shaken this area at shaking intensities of MM8 to MM9.

A3.1.4 Hastings (MM9)

Only one report from Callaghan (1933) mentioned fissures opening in the streets of Hastings. Ground damage was also reported from areas near Hastings, to the south and east, near the old course of the Ngaruroro River (Hancox et al. 1997). The water-mains in Hastings sustained very little damage apart from subsidence at bridges and in earth fills. The sewerage system also suffered only minor damage (Brodie & Harris 1933). The water table in Hastings was particularly low, having experienced a long spell of dry weather (Callaghan 1933), which may help explain the lack of liquefaction effects in the Hastings area.

A3.1.5 Heretaunga Plains (MM9)

The Heretaunga Plains, particularly between Napier and Hastings was criss-crossed by fissures (Conly 1931), particularly on the swampy country and the land skirting rivers between Havelock and Hastings (Baird 1931). Henderson (1933) noted that during and after the earthquake, large quantities of water, sand and silt issued from these fissures, resulting in the flooding of low paddocks near Hastings (Pakowai Road) (Baird 1931). There had been no rain since the earthquake, and before the earthquake the paddocks had been dry. Mud boils were reported under the floorboards of Tuckers Woolsavour at Clive, and at Longlands, a few kilometres to the west of Hastings in the old river bed of the Ngaruroro River (near Irongate Stream) (Fairless & Berrill 1984).

The first span of many bridges had fallen, and built up approaches had slumped due to lateral spreading (Baird 1931). Many of the stop-banks alongside the rivers slumped and were extensively fissured (Callaghan 1933).

The earthquake cut all road communications between Napier and Hastings and the remainder of New Zealand, except for SH2 south towards Wellington. This road was, however, seriously damaged by fissures wherever road embankments had been made across hollows or swamps (failure of the foundation materials in shear), and by destruction of approaches to bridges and culverts (settlement of fills). The general road system in the Hawke's Bay flat country was affected, but not seriously enough to prevent the ready movement of traffic within the area.

On the coast between the Tukituki River and the Ngaruroro River, the lagoons and marshes increased in area such that the salt water damaged crops and pastures previously beyond its reach. The land here was reported to have sunk by approximately 1 foot (~300 mm), and was attributed to the settlement of loose detrital material by the earthquake shaking (Marshall 1933).

Most of the ground damage appears to have occurred to the east of Hastings, with only minimal damage to the west (the sand boils at Longlands being the only identified location). Dellow et al. (1999) attributed this uneven damage distribution to:

1. The change in grainsize distribution across the plains, with the coarser sediments to the west less susceptible to liquefaction-induced ground damage, and the finer grained sediments to the east more susceptible.
2. The attenuation of the intensity of ground shaking from east (MM10) to west (MM8).

The combination of these two factors produced a dramatic change in the nature and extent of observed ground damage. The most severe ground damage occurred to the north of the present course of the Tutaekuri River. A zone of intermediate damage occurred from the present course of the Tutaekuri River south to a line running approximately northwest – southeast through Tomoana. To the southwest of this line ground damage on the Heretaunga plains was largely confined to modern and recent river channels.

A3.1.6 Waiohiki to Puketitiri (MM8–9)

The descriptions of liquefaction-induced ground damage here are somewhat vague, but are included to give the reader some idea as to the style of ground damage that may be expected in this area. To the north of Hakowhai, the main damage was on fill, in cuttings, and in gullies with streams. Several of these gullies showed many long fissures (incipient lateral spreading?), dry gullies had been less affected (Baird 1931).

From Hakowhai to Rissington the damage occurred in patches. Road fillings suffered most near Rissington, and except for minor increases on cuttings and spurs, the damage tapered off towards Puketitiri (Baird 1931). Near Waiohiki, fissures were observed running along gullies at the foot of the hills (possibly basin edge effects). The golf course at Waiohiki was greatly damaged by large and frequent fissures that indicate incipient lateral spreading here at MM9 (Baird 1931).

A3.1.7 Poukawa, Te Aute, Otane, Waipawa, and Waipukurau (MM7–8)

The reports of ground damage in this area indicate that liquefaction-induced ground damage was moderate, with extensive fissuring and settlement occurring in the sedimentary basin that runs north from Waipawa to Poukawa. This basin is accumulating fine-grained sediment and has a water table very close to the surface. The damage to the railway line noted by Callaghan (1933) appears to be largely the result of foundation failure and is very similar in style (but not severity) to the damage that occurred in the Ahuriri lagoon.

A3.1.8 Westshore to Mohaka (MM8)

The liquefaction-induced ground damage north of the Ahuriri lagoon was largely confined to near the mouths of the major rivers. The reports describe sand boils occurring in the lagoon and estuary area of the Mohaka and Te Ngaru (Tangoio) rivers, and near Petane. During and after the earthquake, large quantities of water, sand, and mud issued from fissures in the alluvial flats (Henderson 1933). Liquefaction may also have occurred at some of the more isolated river mouths, but it may not have been observed.

A3.1.9 Wairoa (MM8)

There are few reports of liquefaction at Wairoa, however, water in the lagoon north of Wairoa was reported to have invaded marram grass on the edge of the swamp, and water and/or sand ejection may have occurred (Baird 1931). Callaghan (1933) reported that many of the roads in the area were fissured. A mud spring was reported from Hangaroa, in the Gisborne District.

A3.2 WAIROA EARTHQUAKE OF 16 SEPTEMBER 1932

The M_s 6.9 Wairoa earthquake (Dowrick & Smith 1990) followed nineteen months after the 1931 Napier earthquake. The shaking intensity in Wairoa was estimated to have been MM9–10, in Napier MM6–7, while at Hastings it only reached MM5–6 (Downes 1995). The earthquake was felt strongly over a large part of Hawke's Bay. A description of the effects of this earthquake is given in Ongley et al. (1937). In Wairoa and Gisborne many buildings were badly damaged, and the Wairoa Bridge, damaged beyond repair in the 1931 earthquake, collapsed completely. The earthquake caused extensive fissuring, slumping and landslides, some large, especially around Wairoa and in the country to the northeast of Wairoa.

Some fissuring and cracking of the ground was reported near Wairoa (Hancox et al. 1997). This included a fissure about 6 metres back from the frontage of Marine Parade. It was also reported that the whole business district of Wairoa moved 50–75 mm towards the river. The fissure that this movement occurred on, and other cracks and fissures in the district, widened during subsequent aftershocks. Another newspaper account (Hawke's Bay Herald; 17 September, 1932) refers to "numerous cracks in all the streets, a feature which did not occur in the 1931 shocks". A report from Frasertown (Hawke's Bay Herald, 17 September, 1932) describes the roads as being cracked in every direction. The railway line from Wairoa to Whakaki was badly buckled in numerous places. Newspaper accounts (Hawke's Bay Herald, 17 September, 1932; Dominion, 17 September, 1932) also include reports of "hundreds of miniature geysers" on the Mahia back road, which could be interpreted as sand boils.

Table A3.1 Observations of liquefaction effects reported in the Hawke's Bay region during historical earthquakes. Sources include Hancox et al. (1997), Downes (pers. comm.), and GNS files (from Dellow 1999).

Locality	Modified Mercalli Shaking Intensity				
	6	7	8	9	10
Wairoa – Mohaka	1904 – No liquefaction reported. 1914 – No liquefaction reported.	1921 – No liquefaction reported. 1932 – Minor sand boils near Opoutama – Mahia back road. (Mahia Peninsula isthmus).	1931 – Sand boils on Wairoa flats. Settlement of lagoonal deposits north of Wairoa. 1932 – Whole of the kerbing of the Marine Parade badly fractured. Business district moved 50–75 mm toward river (lateral spread). Subsidence in business area of 50–75 mm. Numerous cracks in all the streets. Country roads cracked in every direction. Harbour wharves damaged. Roads cracked in Frasertown.	1931 – Sand boils near Mohaka River mouth. 1932 – Railway line from Wairoa to Whakaki badly buckled in numerous places. Sand boils and fissures at Marumaru and Opoiti.	
Napier – Taradale		1863 – Liquefaction along banks of Pirimu Stream. Road to spit cracked (Port Ahuriri). 1904 – Land at Whare-o-maraenui badly cracked with sand boils. Sand boils on the left bank of the Tutaekuri River between Taradale and Meanee. Crack in breastwork at Port Ahuriri. 1914 – No liquefaction reported. 1921 – No liquefaction reported.			1931 – Ground fissures Napier South. Westshore embankment broken in many places. Fissures run through many Napier streets either longitudinally or across. Fissures particularly well marked along the present and old infilled channel of the Tutaekuri River, roads were split, water and sewer pipes were ruptured and houses displaced (lateral spreading). Sand boils at Petane and Tangoio Lagoon. Wharf areas at Port Ahuriri badly fissured and collapsed.
Flaxmere – Hastings – Havelock North	1855 – Possible fissure on Heretaunga Plains (near Clive?). Possible gas ejection from swampy ground near Waitangi Creek (Clive). 1914 – No liquefaction reported.	1904 – No liquefaction reported from Hastings – Havelock North area. 1921 – No liquefaction reported.	1863 – Banks of the rivers broken up.	1931 – The whole of the country between Napier and Hastings crisscrossed by fissures, some of them wide and very ugly. Slumping and fissuring of stop banks. Fissures opened along the river channels, especially where these crossed the Heretaunga Flats. The swampy country and that skirting rivers between Havelock and Hastings showed many fissures. At Waiohiki fissures large and frequent with sand boils. Near Hastings low paddocks seen with water in them (sand boils).	
Waipukurau – Waipawa – Otane	1921 – No liquefaction reported from Waipukurau-Waipawa area. 1934 – No liquefaction reported from Waipukurau-Waipawa area. 1990 – No liquefaction reported from Waipukurau-Waipawa area.	?1855 – No data. 1904 – Sand boils and fissures reported in old bed of Waipawa River near Otane. Crack in road between Te Aute and Te Hauke. Liquefaction at Wanstead. 1914 – No liquefaction reported. 1934 & 1990 – No liquefaction reported at Porangahau.	1904 – Liquefaction reported at Porangahau. 1931 – Railway line bent and twisted in many places, embankments slumped. Travelling Waipawa to Hastings a good many fissures were seen when the road adjoined hilly country or crossed waterlogged expanses. No ground damage reported from Waipawa or Waipukurau townships.	Large cracks opening in alluvium.	

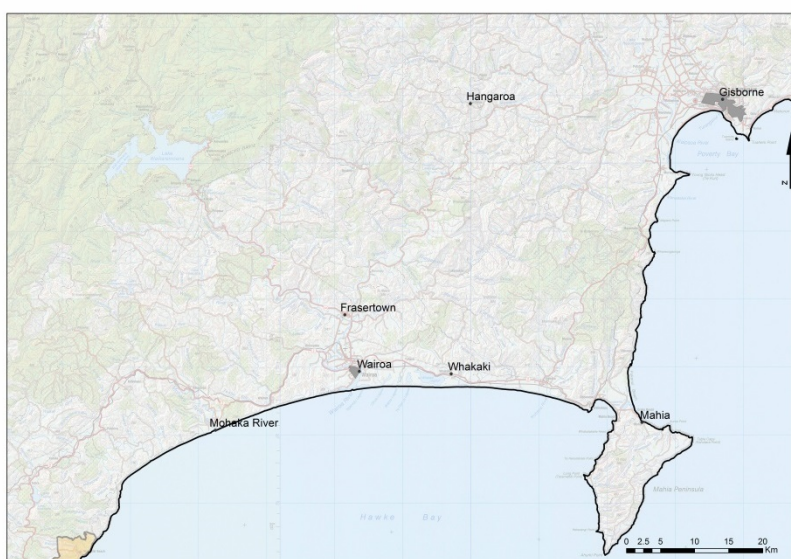
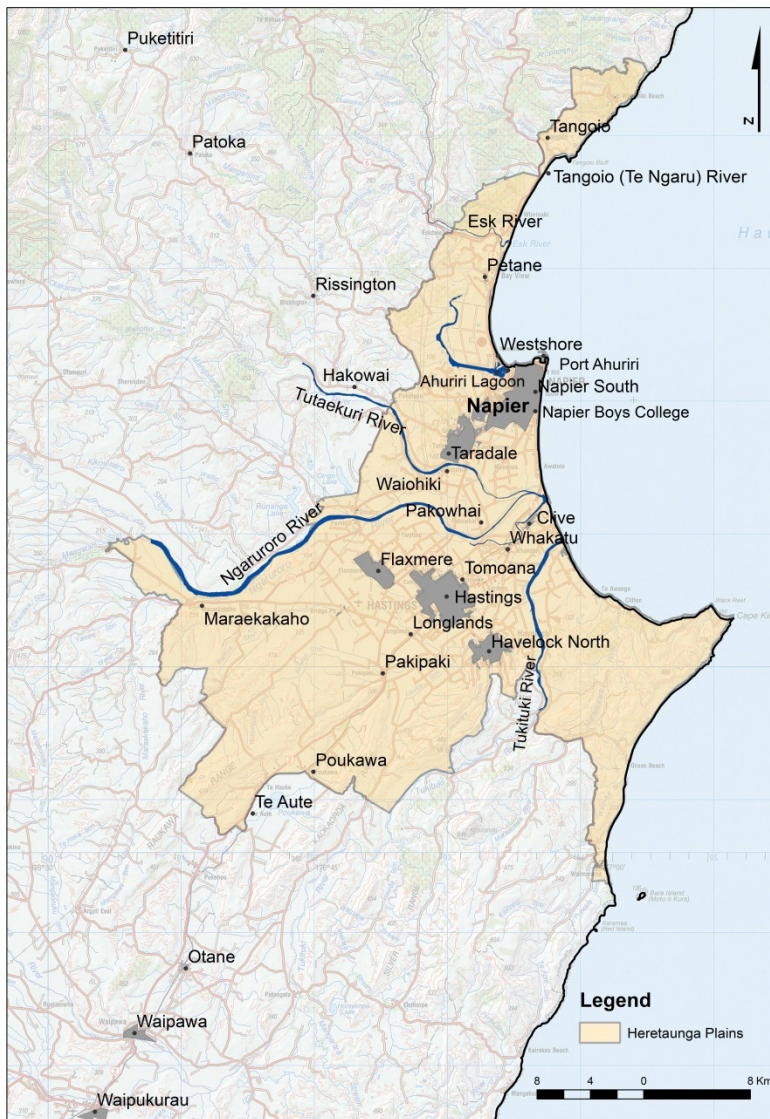


Figure A3.2 Locations of place names used in this Appendix.

A3.3 REFERENCES

- Baird HF. 1931. The Hawke's Bay earthquake of 3 February 1931. Unpublished Report of the Christchurch Magnetic Observatory.
- Brodie A, Harris AG. 1933. Damage to buildings. *New Zealand Journal of Science and Technology*. 15(1):108-115.
- Butcher HF. 1931. General description of the Napier-Hastings earthquake, 3rd February, 1931. *Community Planning*. 1(3):86-89.
- Callaghan FR. 1933. The Hawke's Bay Earthquake, General description. *The New Zealand Journal of Science and Technology*. 15(1):3-37.
- Conly DG. 1931. Hawke's Bay: Before and After: The great earthquake of 1931: an historical record. Napier: Daily Telegraph Company.
- Dellow GD, Hengesh JV, Heron D, Brown L, Hull AG. 1999. Earthquake Hazard Analysis Program: Stage II: Part II – Evaluation of Liquefaction Potential in the Hawke's Bay Region. Lower Hutt: Institute of Geological and Nuclear Sciences Limited (Contract Report 33591.D. Client Report 1999/6). Prepared for Hawke's Bay Regional Council. March 1999. 63 p.
- Downes GL. 1995. Atlas of isoseismal maps of New Zealand earthquakes. Lower Hutt: Institute of Geological and Nuclear Science. 304 p. (Institute of Geological and Nuclear Sciences monograph; 1).
- Dowrick DJ. 1998. Damage and intensities in the magnitude 7.8 1931 Hawke's Bay, New Zealand, earthquake. *Bulletin of the New Zealand National Society for Earthquake Engineering*. 31(3):139-136.
- Dowrick DJ, Smith EGC. 1990. Surface wave magnitudes of some New Zealand earthquakes 1901-1988. *Bulletin of the New Zealand National Society for Earthquake Engineering*. 23(3):198-210.
- Fairless GJ, Berrill JB. 1984. Liquefaction during historic earthquakes in New Zealand. *Bulletin of the New Zealand National Society for Earthquake Engineering*. 17(4):280-291.
- Hancox GT, Perrin ND, Dellow GD. 1997. Earthquake-induced landsliding in New Zealand and implications for MM intensity and seismic hazard assessment. Lower Hutt (NZ): Institute of Geological & Nuclear Sciences. (Institute of Geological & Nuclear Sciences client report; 43601B).
- Hancox GT, Perrin ND, Dellow GD. 2002. Recent studies of historical earthquake-induced landsliding, ground damage, and MM intensity in New Zealand. *Bulletin of the New Zealand Society for Earthquake Engineering*. 35(2):59-95.
- Henderson J. 1933. The Hawke's Bay earthquake, Geological aspects of the Hawke's Bay earthquake. *New Zealand Journal of Science and Technology*. 15(1):38-75.
- Hull A. 1990. Tectonics of the 1931 Hawke's Bay earthquake. *New Zealand Journal of Geology and Geophysics*. 33:309-320.
- Marshall, P 1933. Effects of earthquake on coast-line near Napier. *The New Zealand Journal of Science and Technology*. 15(1):79-92.
- McSaveney E. 'Historic earthquakes - The 1931 Hawke's Bay earthquake', Te Ara - the Encyclopedia of New Zealand. [accessed 2017 Sep 07] <http://www.TeAra.govt.nz/en/historic-earthquakes/page-6>.
- Ongley M, Walshe HE, Henderson J, Hayes RC. 1937. The Wairoa Earthquake of 16th September, 1932. *New Zealand Journal of Science and Technology* 18(12):845-865.

A4.0 GEOLOGICAL AND GEOMORPHOLOGICAL MAPPING DATA

A4.1 GEOLOGICAL SETTING

New Zealand lies along the margins of two tectonic plates, the Indian-Australian Plate and the Pacific Plate (e.g., Beavan and Haines 2001; Dravid and Brown 1997; Walcott 1978). The boundary between these two plates is characterized by faulting, folding and associated seismological and volcanological activity.

The Hikurangi Trough lies 100–200 km east of Hawke's Bay and is the eastern margin of the Indian-Australian and Pacific plate boundary. The plate interface has its surface expression in the Hikurangi Trough and dips westwards from the Hikurangi Trough beneath Hawke's Bay and the Heretaunga Plains in the form of a gently dipping mega-fault that separates the down-going slab of oceanic crust (the Pacific Plate) from the overlying Australian Plate. Beneath the Heretaunga Plains the plate boundary mega-thrust lies at a depth of c. 20 km (Barker et al. 2009; Wallace et al. 2009). This segment of the plate boundary became active at the start of the Miocene (around 23 million years ago) and since then has been the locus of tectonic activity, including episodic uplift and subsidence in different parts of the east coast of the North Island at different times, resulting in localised marine basins with thick deposits of mudstone and sandstone. Contraction between the tectonic plates during the Pliocene resulted in more uplift, and limestones were deposited along the margins of a seaway that stretched from Hawke's Bay to Wairarapa. The southern end of the seaway connection was closed by the end of the Pliocene and the resulting embayment was filled rapidly by terrestrial deposits eroded from the nearby uplifting axial ranges. Tephra beds in early Quaternary rocks record volcanic activity from the Taupo Volcanic Zone (TVZ) that began around 2 million years ago; a particularly large eruption 1 million years ago deposited ignimbrite almost as far as Cape Kidnappers. At around the same time, thick marginal marine to non-marine gravels were deposited around Cape Kidnappers and other areas of Hawke's Bay. Much of the Hawke's Bay land area had emerged from the sea by around 1.7 million years ago.

The Heretaunga Plains have formed as the result of a complex interaction between tectonics and glacio-eustatic sea-level changes during the Quaternary (last two million years). The interpretation of the stratigraphy beneath the Heretaunga Plains used here relies on a well-tested geological model based on continuing deposition within a tectonically deforming (subsiding) basin through the cyclical global climatic changes of the Quaternary Period. Through the Quaternary, cyclical global climatic changes have involved climatic fluctuations (approximate periodicity of 100 000 years) between glacial (cold) events and interglacial (temperate) periods. A result of this climate change was glacio-eustatic sea level fluctuation that ranged from a few metres above the current sea level (during warm periods, such as today) to 130 m below (during the extreme glacial periods, the last of which culminated c. 20 000 years ago; (Pillans et al. 1998; Siddall et al. 2003; Rabineau et al. 2006). Because the Heretaunga Plains has been continuously subsiding during at least the last 250 000 years (Dravid & Brown 1997; Beanland et al. 1998) at a rate of c. 1 m/1000 years, its sedimentary history reflects these glacial – interglacial cycles.

Warm climatic cycles were characterised by high sea levels, sediment carrying capacity of rivers was low (as stream gradients were low close to the coast of the day), and deposits were fine-grained. During cold climatic cycles, sea level was low, frost-related erosion in the high country was high, sediment supply to the major rivers was high, and river gradients at the Heretaunga Plains were relatively steep, because the coastline was distant near the edge of the continental shelf. Because the basin was subsiding, broad gravel plains were deposited by the braided rivers

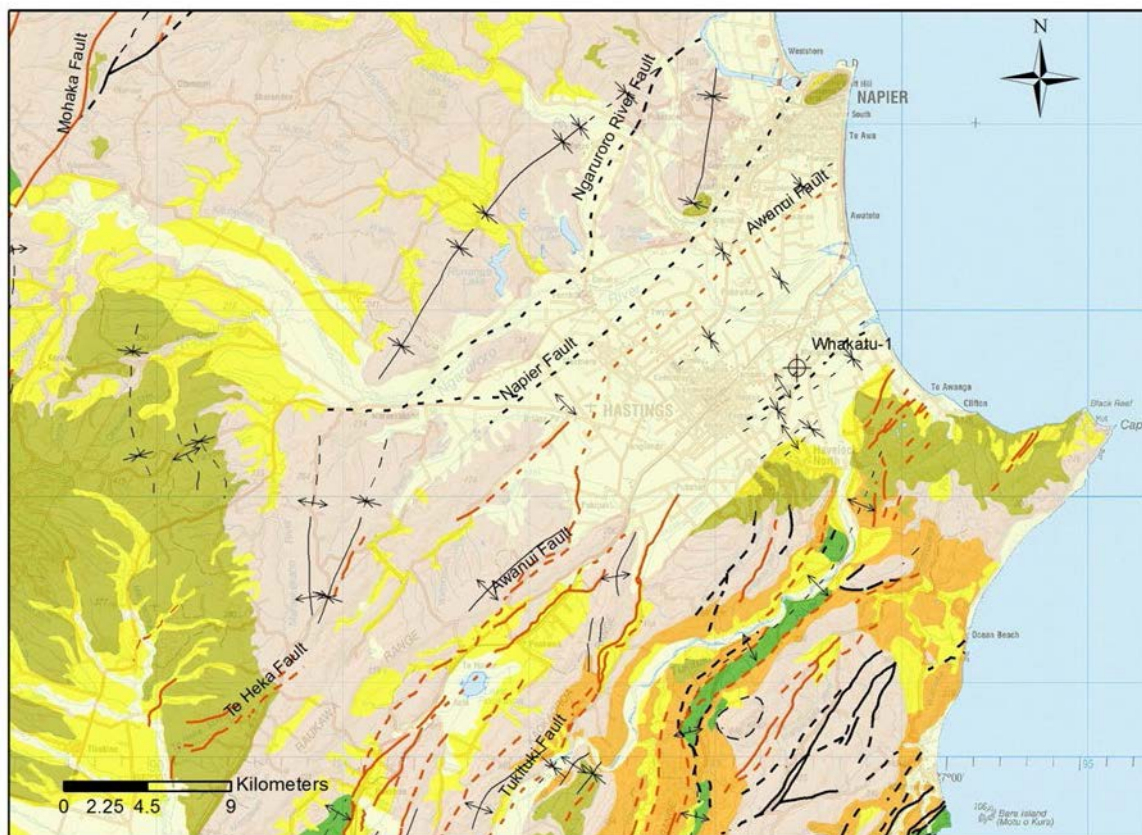
of the day. This has resulted in a complex sequence of river channel and flood plain deposits overlying shallow marine sediments. Flood plain sediments deposited in the last 10 000 years are up to 20 metres thick, with shallow marine sediments thickness ranging from 0–40 metres (Dravid & Brown 1997). It is these shallow (to a depth of twenty metres), fine-grained sediments of the Heretaunga Plains, deposited since the end of the last glaciation 10,000 to 14,000 years ago that are susceptible to liquefaction today.

Early Quaternary geological units in the Havelock North area dip beneath the Heretaunga Plains (Figure A4.1), while those of the north side of the plains dip gently south-eastwards beneath the flat land. Using subsurface data Dravid and Brown (1997) and Beanland et al. (1998) concluded that the Heretaunga Plains area represents a tectonically controlled depression between 900 m and 1600 m deep. A series of active faults extend from the Waipukurau area northeast to the southern margin of the Heretaunga Plains (Kelsey et al. 1998), and the Awanui and Tukituki faults most likely continue beneath the plains (Figure A4.1). Seismic reflection data suggest that faults, such as the Ngaruroro River and Napier faults, lie at depth beneath the Quaternary sediments (Beanland et al. 1998; Dravid & Brown 1997).

After the most recent large eruption from Lake Taupo c. 1800 years ago, large quantities of Taupo Pumice Alluvium built up rapidly on the Heretaunga Plains. The pumice has been eroded in some places by alluvial processes, but up to 10 m thickness of pumice gravel and sand are found in many parts of the plains. Aggradation of the rivers has continued since the pumice deposition, with a further 5–10 m of alluvial sediment overlying the pumice in parts of the Heretaunga Plains. This thick accumulation of very young deposits provides conditions that are likely to create high susceptibilities to liquefaction in this area.

The youngest (Holocene; <10,000 years old) fluvial sediments of the Heretaunga Plains, comprise interfingered layers and lenses of sand, silt and gravel. The estuarine deposits near Napier (Figure A4.5) appear to form a shallow veneer (up to 40 metres) of soft sediments which overlie the interlayered fluvial deposits (up to 20 metres thick) of the Heretaunga plains (Dravid & Brown 1997). These in turn are overlain by coarse sands and gravels of the beach deposit (up to 20 metres thick) along Marine Parade in Napier (Dravid & Brown, 1997). At Wairoa, subsurface investigations (Ota et al. 1989) show up to 30 metres of recent (post-glacial) fine sands and deposited in an estuarine environment.

A generalised geology map is shown in Figure A4.1.



Legend

Geology	Active Faults	Folds (inactive)
Holocene	— Accurate fault	↑ ↓ accurate, anticline
late Quaternary	- - - Approximate fault	— * accurate, syncline
early Quaternary	- - - Concealed fault	- - - ≈ approximate, anticline
Pliocene	- - - Inferred fault	- - - ↑ ↓ approximate, monocline bedding limbs dipping
Miocene		- - - * approximate, syncline
Rocks older than Miocene		- - - ≈ concealed, anticline
Whakatu-1 petroleum well		- - - ↑ ↓ concealed, monocline bedding limbs dipping
		- - - * concealed, syncline
Inactive Faults		
	— Accurate fault	
	- - - Approximate fault	
	- - - Approximate thrust	
	- - - Concealed fault	
	- - - Concealed thrust	
	- - - Inferred fault	

Figure A4.1 Generalised geological map of the Heretaunga Plains, divided into undifferentiated units older than Miocene, Miocene, Pliocene, Quaternary and Holocene. The geology is structurally complex as faulting and folding occurred episodically throughout the Pliocene and Quaternary. "Accurate", "approximate", "concealed" and "inferred" refer to the accuracy of the location of the fault or fold (see section on Uncertainties). Adapted from Lee et al. 2011.

A4.2 TERRAIN MODELS

High quality Light Detection and Ranging (LiDAR) digital elevation models and derivative hill shade images provide a very high-resolution depiction of the form of the ground surface. They provide a basis for the interpretation of the nature and origin of landforms, which, in turn, provides a basis for inferring the likely character of the underlying geological materials.

LiDAR data has been captured in 2003, 2006 and 2011–12 for the Hawke's Bay Regional Council. Data captured in 2003 and 2006 covers most of the study area except for the upper reaches of the Ngaruroro River. The original data had a 10 m offset, with sea level set at 10 m. Cell values were recalculated by subtracting 10 from each cell to normalise sea level to zero. A combined elevation model of the 2003/2006 and 2011–12 with a 1 m resolution was built by William Ries (GNS Science) using the IDW algorithm. To reduce the file size, the 1 m resolution model was reprocessed to 2 m. Gaps in the data were filled using the focal statistics algorithm in ArcGIS.

The 2003 metadata sheet for this LiDAR data states that the horizontal accuracy of each laser strike was <0.55 m and the vertical accuracy was around 0.15 m. Ground elevations beneath trees may be less accurate, although no uncertainty estimate is supplied. Field checks of the LiDAR survey showed there is less accuracy in the Te Aute area, with a standard deviation of 0.509 m and no test points were surveyed in some areas. Horizontal accuracy of the 2006 laser strikes has a horizontal accuracy of <0.4 m and a vertical accuracy of 0.15 m. Again, ground elevations beneath trees may be less accurate. The 2003 and 2006 LiDAR data were merged and there are height variations in places such as riverbeds and agricultural crops. The LiDAR files were delivered as xyz point data and processed to create gridded elevation models at 2 m resolution. However, due to the low density of the data, actual resolution is more likely to be accurate to 5 m.

The elevation model was further reprocessed to a lower resolution when imported into Leapfrog. It is not possible to import LiDAR data with large file sizes (e.g., the LiDAR data for the study area was 3.57GB) at high resolutions (such as 2 m), as the software is unable to process this data efficiently. The resolution of the elevation model in Leapfrog is based on triangulation of the surface rather than the pixel-based raster resolution in ArcGIS. For this project, the resolution of the elevation model in Leapfrog was set to 50.

Outside of the LiDAR area, collar heights for borehole and geotechnical probing (including Cone Penetration Test (CPT)) data were extracted from an 8 m resolution elevation model (created by Geographx; www.geographx.co.nz). This DEM has a 22 m horizontal accuracy and 10 m vertical accuracy.

A4.3 SOILS AND GEOMORPHOLOGY

The form and origin of the ground surface (geomorphology) provides insight into the nature of the underlying geological materials, and the processes that formed them. Information on subsurface materials provided by records in the borehole database and geotechnical investigations gives information on subsurface materials at discrete locations. The soil and geomorphologic information provides an area-wide, general indication of what lies beneath the near-surface, i.e., within 10 m or so of the ground surface, as well as providing insights into the processes, such as erosion and deposition, that shaped the ground surface.

Landforms on the geomorphic map were largely identified using aerial photography and LiDAR, which was also used as a base map. LiDAR was used to interpret boundaries between geomorphic units, largely using variations in texture and pattern on the high resolution topographic imagery. Soil maps provide information to distinguish between landforms of coastal and river origin, and allow for the mapping of indicative ages.

The dominant features of the geomorphology of the project area are the recent and abandoned river channels and levees of the Tutaekuri and Ngaruroro Rivers that cover most of the Heretaunga Plains; and the estuary plain of the old Ahuriri Lagoon west of Napier. The hills surrounding the plains are mostly underlain by undifferentiated Pliocene aged rock, and were excluded from the project area as they are not susceptible to liquefaction.

A4.3.1 Soil Map Compilation

Digital soil maps for the Heretaunga Plains were provided by Landcare Research. Soil boundaries were based on those in S-Map, the new digital national soils database of New Zealand ([ihttp://smap.landcareresearch.co.nz/home](http://smap.landcareresearch.co.nz/home)), which was interrogated to produce maps of soil group, soil age and profile drainage (including identifying those soils with a pan that might affect drainage) (<http://dx.doi.org/10.7931/L1WC7>). The soil maps were produced by amalgamating soil maps for the Heretaunga Plains produced by Griffiths (2001, 1996), with soil maps of Hastings and Havelock North urban areas produced by Wilde et al. (2006). The surface ages were based on those assigned by Griffiths (2001). Soil maps for the Heretaunga Plains are shown in Figure A4.2 – Figure A4.4.

Soils can provide information relevant to liquefaction for the following reasons:

- Soil Group: groupings based on soil parent material and rock type give us an indication of the materials at the surface; their rock type (or source) and their texture (e.g., alluvial gravels vs. marine sands);
- Soil age: gives an indication of the age of the landform on which the soil developed, to help with geomorphology mapping e.g., defining different ages of abandoned river channels of the Ngaruroro and Tutaekuri Rivers;
- Drainage class: give us an indication of where the water table is high or where drainage is impeded by underlying harder layers (pans).

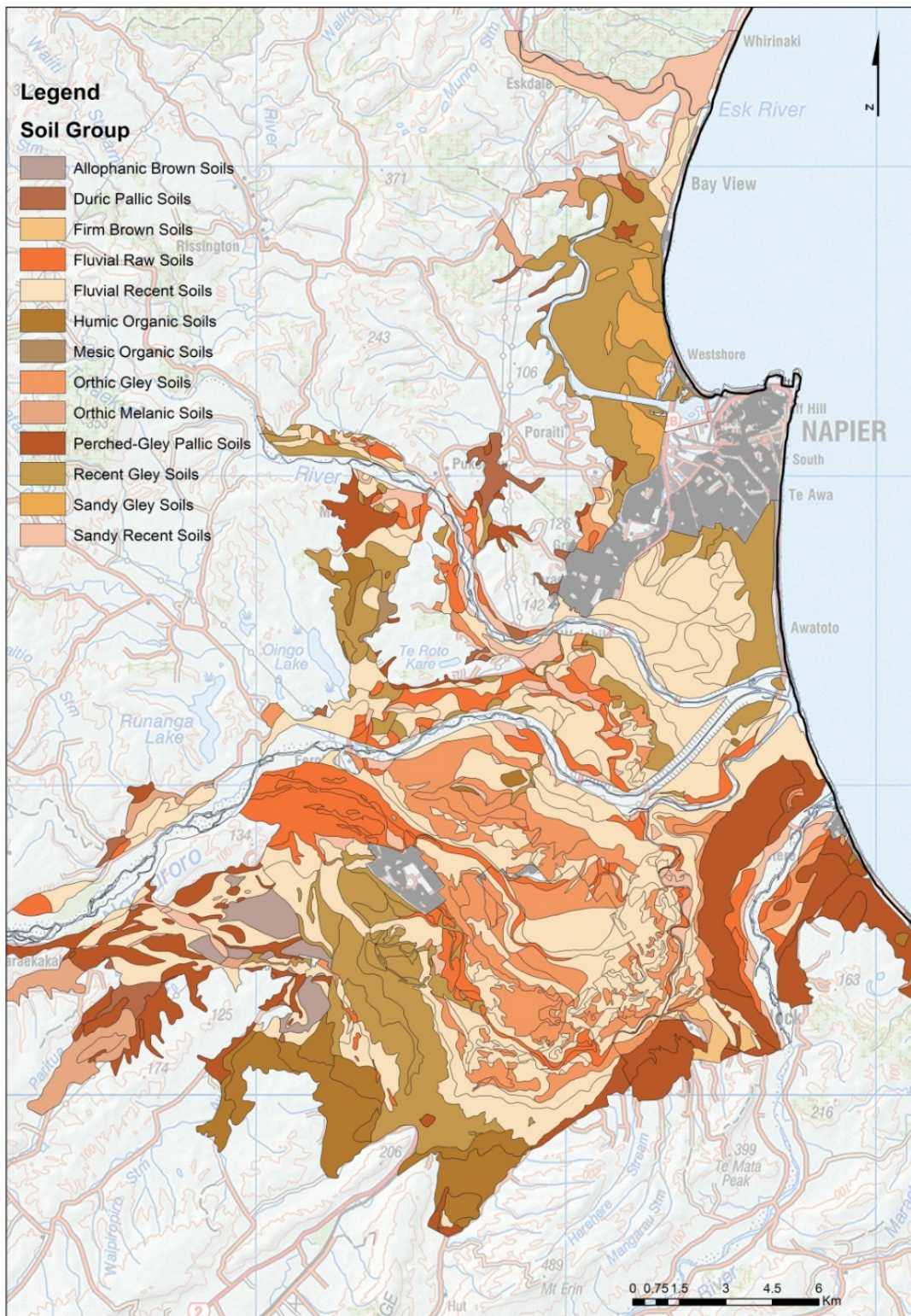


Figure A4.2 Soil Group.

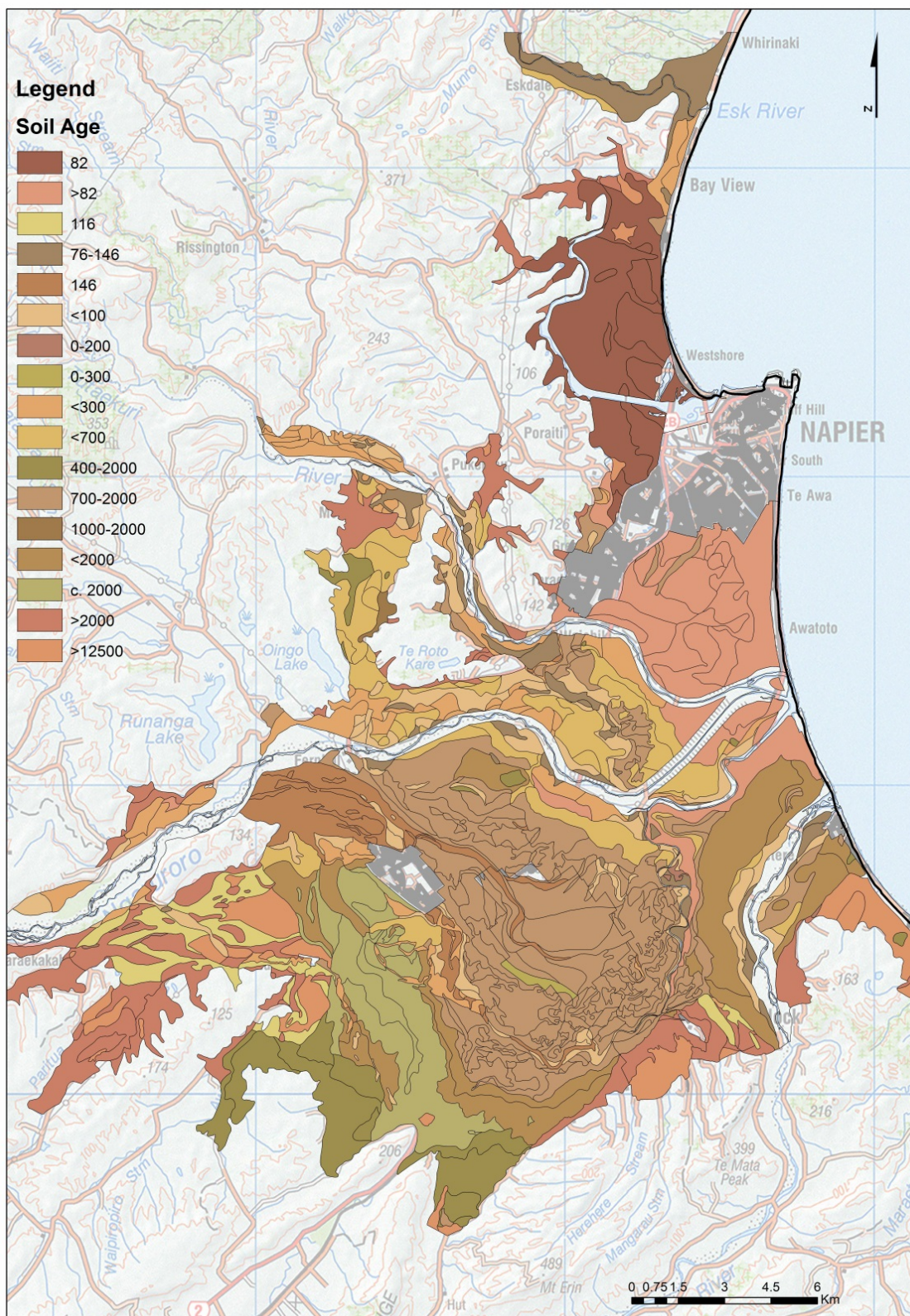


Figure A4.3 Soil Age (in years).

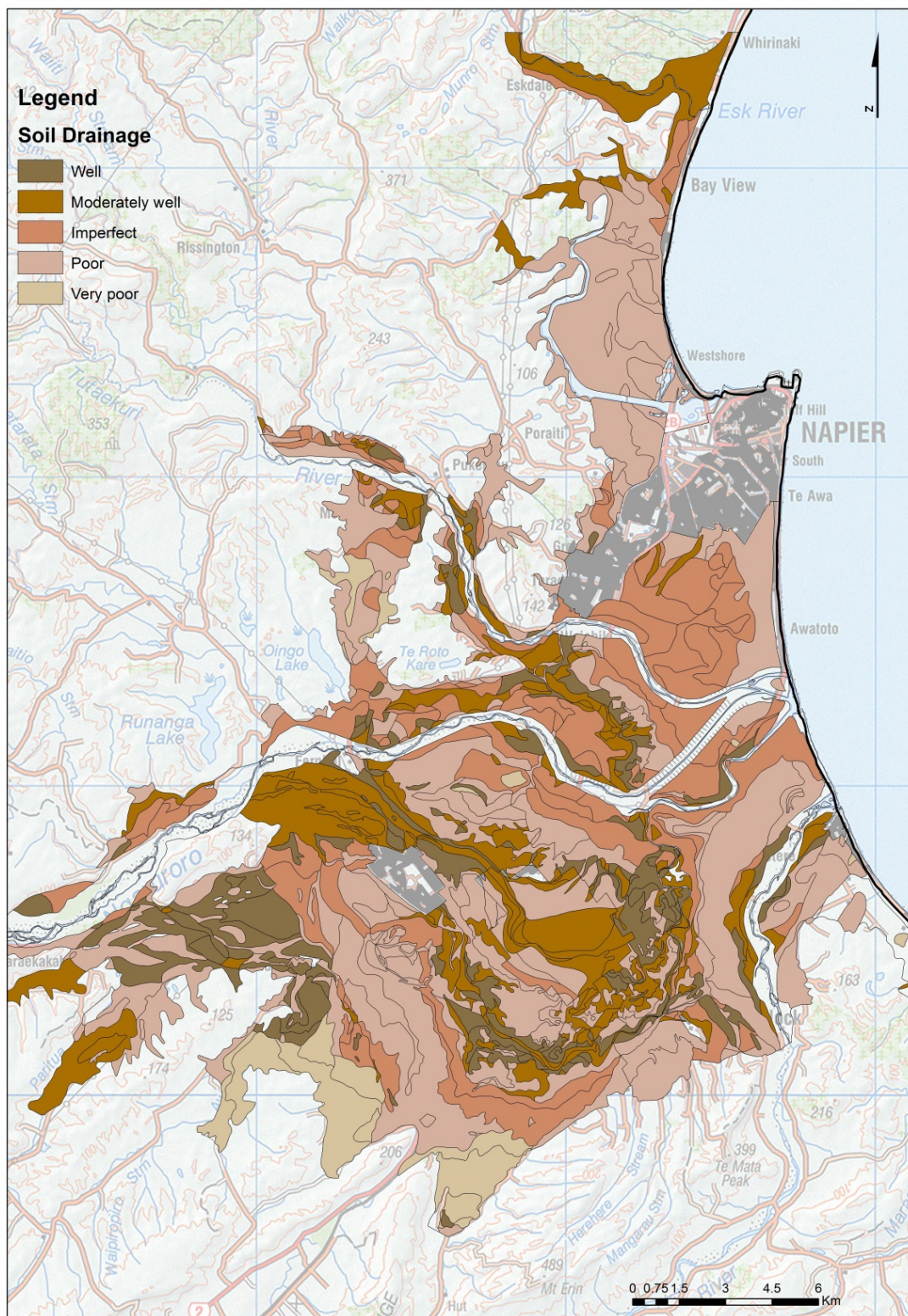


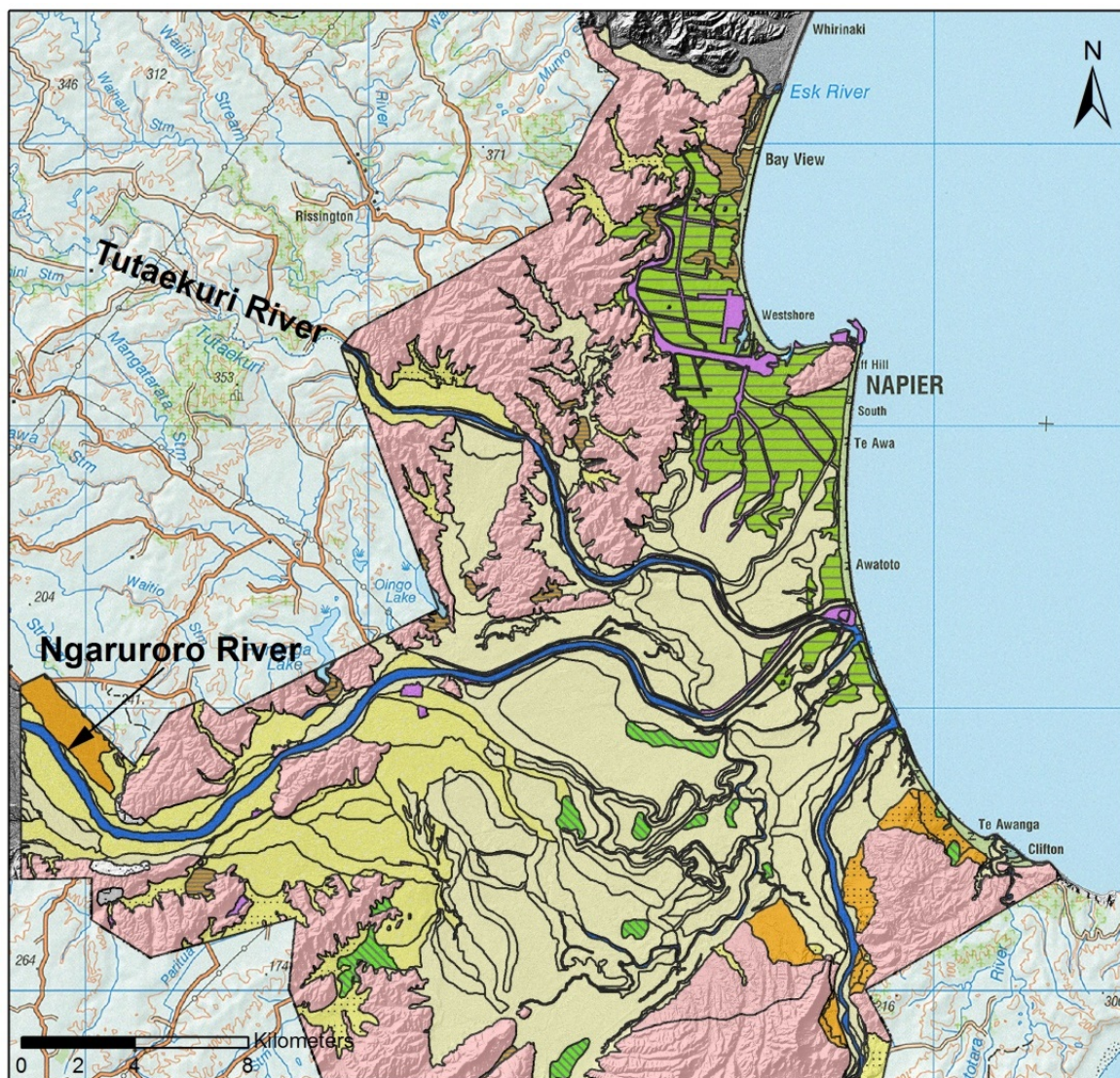
Figure A4.4 Soil drainage class.

A4.3.2 Geomorphology Map

A geomorphology map was developed for the project area. Landforms of the project area were categorised according to their origins and ages, as illustrated in a generalised geomorphic map (Figure A4.5). The categories are divided into:

- Anthropogenic features;
- Dynamic features of the land surface (natural water bodies and river courses);
- Landforms of the Holocene Epoch (around the last 12,000 years), which comprise most of the river, stream, swamp, estuarine and coastal features of the Heretaunga Plains;
- Landforms of the Late Pleistocene epoch created by fluvial processes that were formed during the last glaciation; and
- Landforms of the hill country surrounding the Heretaunga Plains.

Although the surface geomorphology only maps the origin of the surfaces being examined, it provided two elements needed to more finely differentiate the liquefaction hazard. The first was to describe the sedimentary origin of the near-surface sediments (0–5 metres depth). The second was to provide a basis for a more detailed spatial differentiation of the Heretaunga Plains. This detailed spatial differentiation provided a basis for examining liquefaction response using cone penetration test (CPT) data. Polygons with a high density of CPT data and similar liquefaction response can be grouped together and then those with a similar geomorphology, but with few or no CPT data, can be assigned a liquefaction susceptibility that is likely to represent their liquefaction behaviour.



Legend

Dynamic features		Late Pleistocene	
natural water body		river channel raised	
river bed or channel		river flood basin	
Holocene Landforms		Hill country landforms	
beach plain	human drainage channel	river plain	Undifferentiated
beach ridge	human embankment	river plain braided	
depression	human engineered ground	river terrace	
estuary plain	human excavated ground	stream channel	
fan alluvial	human filled ground	stream channel incised	
fan colluvial	human floodbank	stream channel raised	
human constructed wetland	human impounded water body	stream plain	
	human modified estuary plain	swamp	
	landslide terrain	swamp drained	
	river channel		
	river channel incised		
	river channel interflue		

Figure A4.5 A generalised geomorphic landforms map of the Heretaunga Plains area. The dominant features are the recent and abandoned river channels and levees (yellow) from the Tutaekuri and Ngaruroro Rivers that cover most of the plains; and the estuary plain from of the old Ahuriri lagoon west of Napier. The hill country surrounding the plains is mostly underlain by undifferentiated Pliocene aged rock.

A4.4 BOREHOLE DATA

A4.4.1 Distribution

The Heretaunga Plains aquifer system was discovered in the 1860s, and borehole records from that time have been collected and digitised within a database of well-logs and groundwater data (Dravid & Brown 1997). This Hawke's Bay Regional Council borehole database is a collection of 7503 borehole logs that cover the area from Gisborne in the east, the Kaingaroa Forest in the north, and south to the central Hawke's Bay District. The borehole logs database is a valuable resource that contains information on subsurface materials encountered during drilling; it provides data useful for constructing a 3D model of the subsurface materials.

The wells were drilled by many drillers over a long period of time and it is inevitable that their quality varies. Most were drilled at locations that were estimated, sometimes on poor quality base maps. Some logs may have been compiled retrospectively from the driller's memory, and almost all were drilled with the primary purpose of locating the groundwater aquifer. For these reasons, while we recognise that this is an exceptionally valuable database, we regard it as one of heterogeneous quality and reliability, and when using it to interpret stratigraphy, prefer to base decisions on multiple logs rather than individual ones. For this reason, our stratigraphic surfaces do not honour each log, but are a best fit from all available logs in a local area.

The borehole database was clipped to this project's area of interest, the remaining 4108 borehole logs (Figure A4.6) are well distributed over the Heretaunga Plains. Most of the boreholes are less than 50 m deep and more than half are between 20–50 m deep. Some boreholes greater than 100 m depth referenced in Brown (1993) are not present in the HBRC database, but they have been incorporated within the dataset used in modelling.

A4.4.2 Method of Processing

The borehole data within the area of interest was first cleaned to remove duplicate collar files and collar files that were missing lithological interval information. Some collar files with identical grid references had different IDs and interval data; these data were also excluded as it was impossible to assess which data was correct. New borehole collar heights were allocated from LiDAR data and this cleaned data was loaded into Leapfrog Geo. The locations of the boreholes are shown in Figure A4.6.

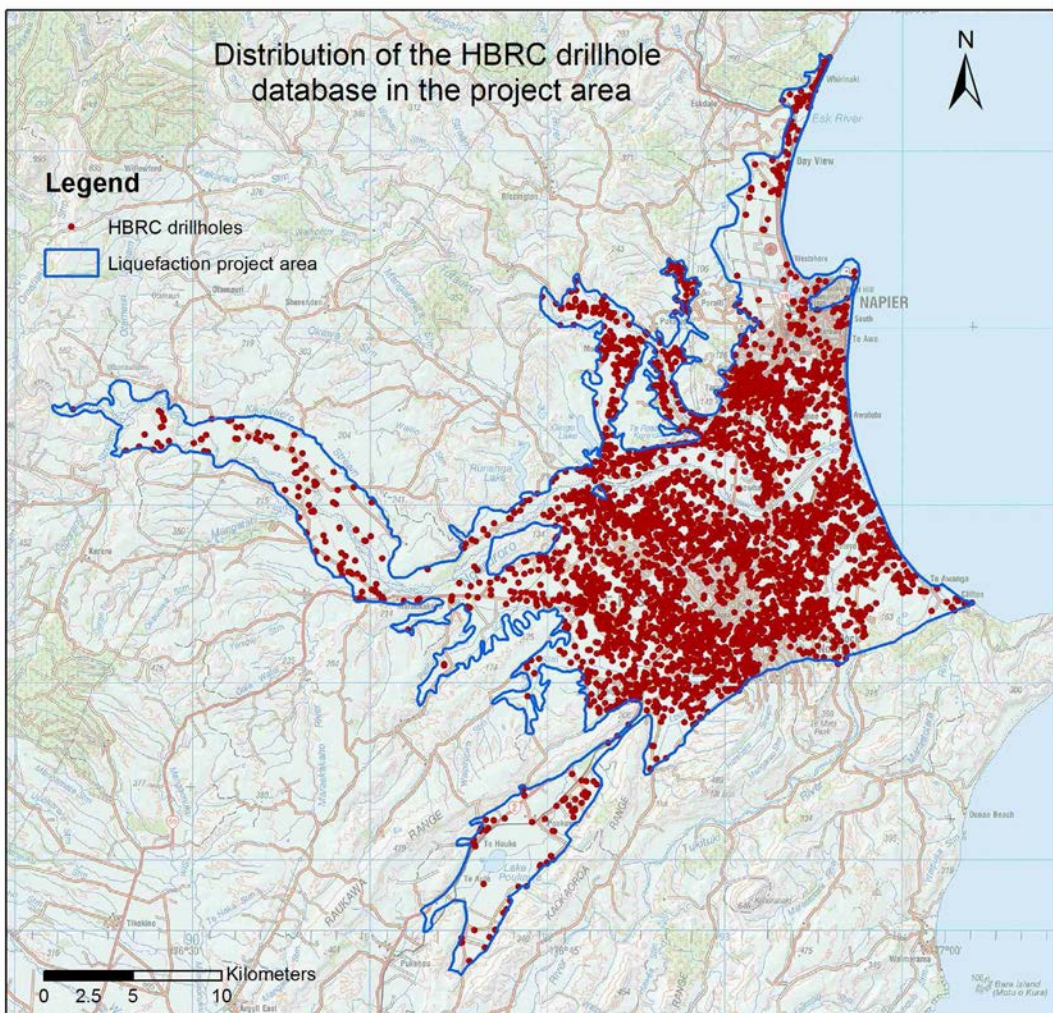


Figure A4.6 The HBRC boreholes have been clipped to the area of the Heretaunga Plains and are well distributed across the Heretaunga Plains.

A4.4.3 Lithological Data from The Borehole Database

The lithological information attached to the borehole data is documented as 'primary strata' and 'full strata' within intervals down the borehole. The 'primary strata' field describes only the main lithology of the sediments within that interval, e.g., gravel, whereas the 'full strata' field contains a description of all lithologies encountered at that interval (e.g., sandy, silty gravel). Lithologies recorded in the 'primary strata' field are mainly gravel, sand, silt, clay, or mudstone.

Once loaded within Leapfrog Geo, patterns of coherent stratigraphy using the primary strata field were identified. Sand, gravel, silt and clay dominate the 'primary strata' field (Figure A4.7). This work shows that gravel can be mapped as coherent stratigraphic units with a strong level of confidence, but in almost all cases, clay, sand and silt records cannot be mapped reliably over any distance. Across the Heretaunga Plains the one characteristic that reliably indicates the presence of Holocene marine is the widespread presence of marine shells. Shells are present locally at depths up to 54 m close to the coast and their maximum depth reduces inland.

Most boreholes terminate at the top of a thick gravel unit at around 30–50 m depth. Radiocarbon ages indicate that this gravel unit is Last Glacial in age (14,000 to 24,000 years old) (Dravid & Brown 1997). Packets of Holocene gravel overlying the Last Glacial gravels (Figure A4.8 and Figure A4.9) have been identified and mapped along the coast south of Napier (Napier beach gravel, Haumoana beach gravel), near the mouth of the Tukituki River (Tukituki fan, Tukituki river mouth fan) and along the Ngaruroro River (Ngaruroro fan).

The detailed characteristics of the Holocene and Last Glacial gravels is provided in the groundwater report on 3D modelling of the Heretaunga Plains for groundwater management (Lee et al. 2014).

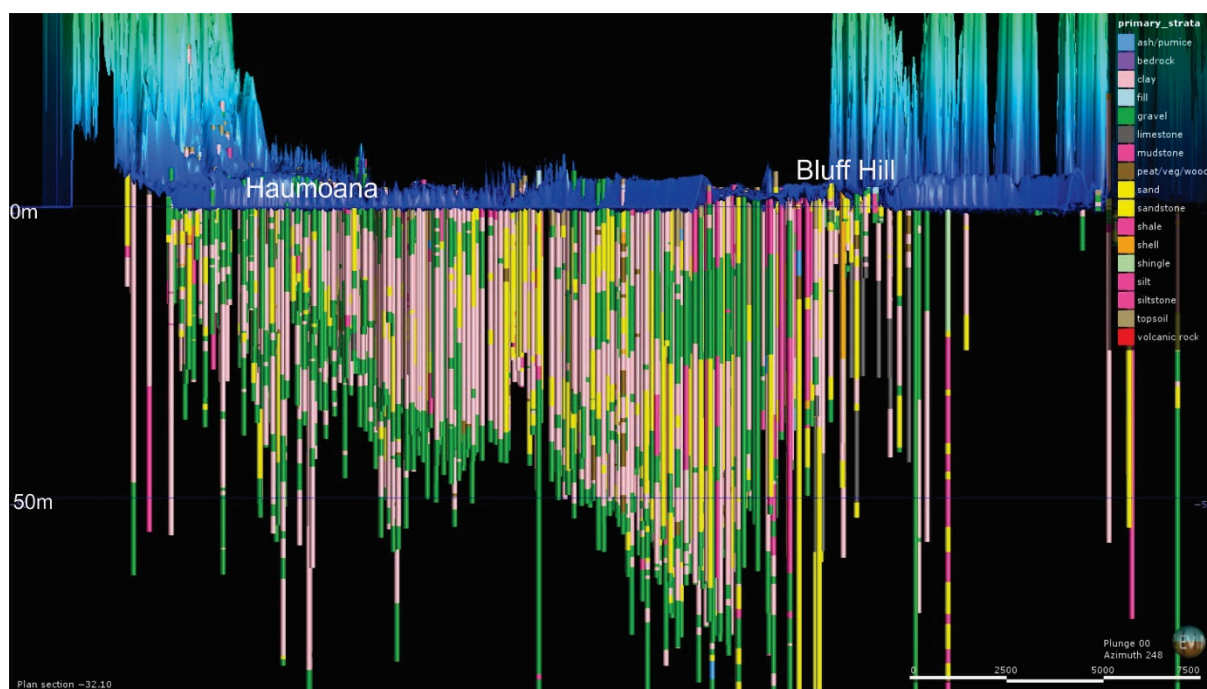


Figure A4.7 A Leapfrog cross section from Haumoana to Bluff Hill in the north. The boreholes show subsurface lithologies are dominated in this area by clay (pink) and gravel (green). Apart from gravel, other units such as sand (yellow) and silt (dark pink), do not display any coherent mappable stratigraphy. The boreholes mostly terminate at the top of the lowermost gravel, which we interpret as Last Glacial in age. Vertical exaggeration is 150.

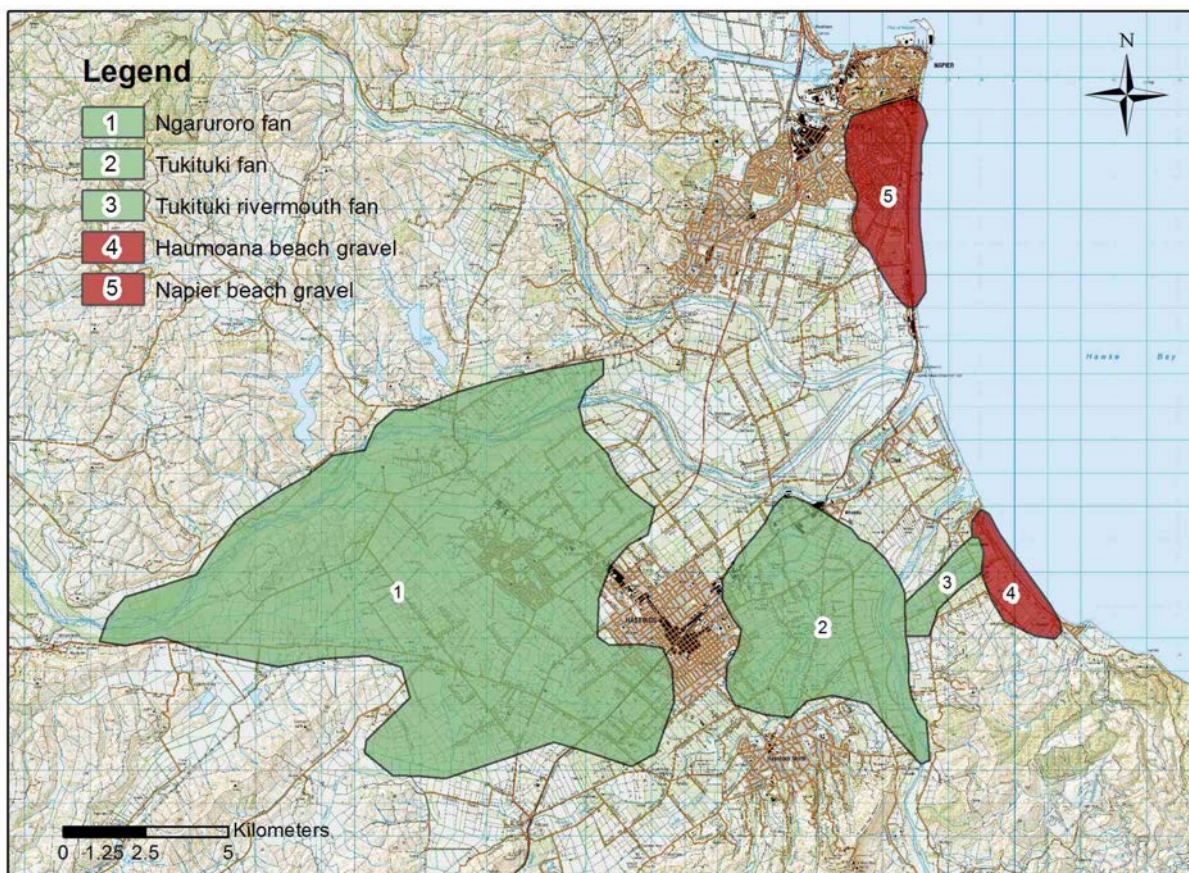


Figure A4.8 A map view of the surface and subsurface distribution of Holocene gravels identified from the boreholes. Beach barrier bar gravels are located south of Napier and at Haumoana (reddish brown). Inland alluvial fan deltas (green) were deposited by the Ngaruroro and Tukituki rivers.

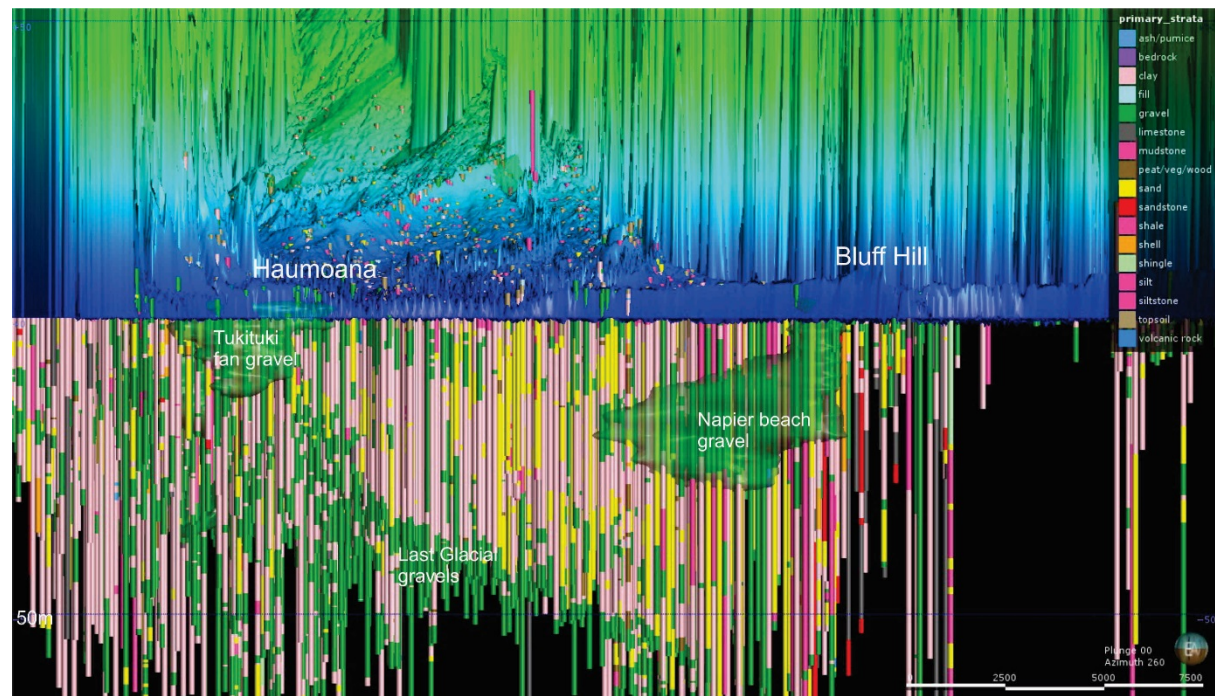


Figure A4.9 A cross section from Haumoana to Bluff Hill shows some of the Holocene gravel units identified using borehole data. The Napier Beach gravels lie between 15–20 m below sea level. Fan gravels deposited by the Tukituki River are found up to 10 m below the ground surface.

The distribution of shells in the borehole data show the sea transgressed inland almost as far as Pakipaki at the end of the period of post-glacial sea level rise c. 7000 years' ago (Figure A4.10). The occurrence of widespread marine shells, locally to depths of ~50 m indicates that enclosing materials are Holocene in age.

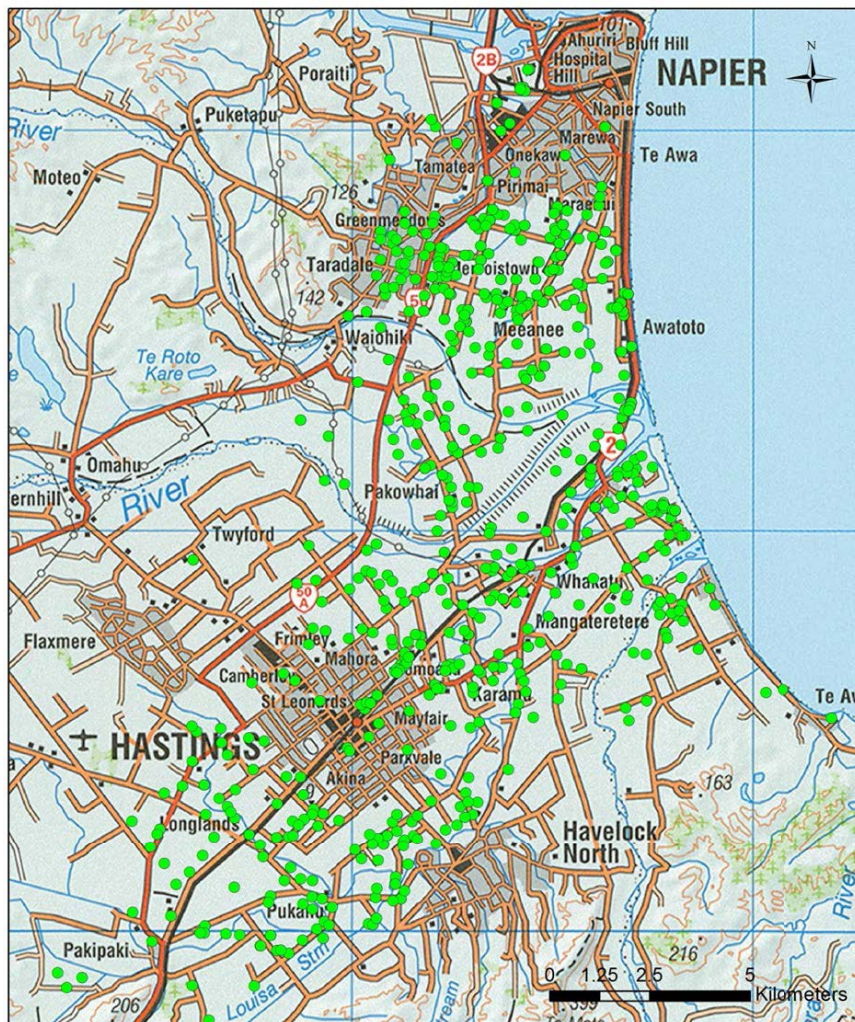


Figure A4.10 The distribution of shells (green dots) from borehole data that lie above the base of the Holocene surface, showing the maximum inland extent of sea level 7000 years ago.

A4.4.4 Mapping Dominant Lithology in Boreholes

While the large number of borehole logs were useful in defining the gravel units, and the extent of Holocene shelly materials, it was necessary to thin the data to use for identifying subsurface lithologies. In trying to characterise the Holocene materials that may liquefy, boreholes in materials of Last Glacial age or older materials were eliminated. The thinning operation was conducted to ensure an even distribution of boreholes across the area (Figure A4.11). Each borehole was summarised into a dominant lithology for each one metre interval to a depth of 10 m; and then as a single unit from 10 to15 m. This depth of 15 m was chosen as representing the deepest extent of liquefiable materials that may be a major contributor to surficial liquefaction (Brackley et al, 2012). The thinned borehole dataset was used in conjunction with the geomorphic map to correlate subsurface materials with surface-forming processes.

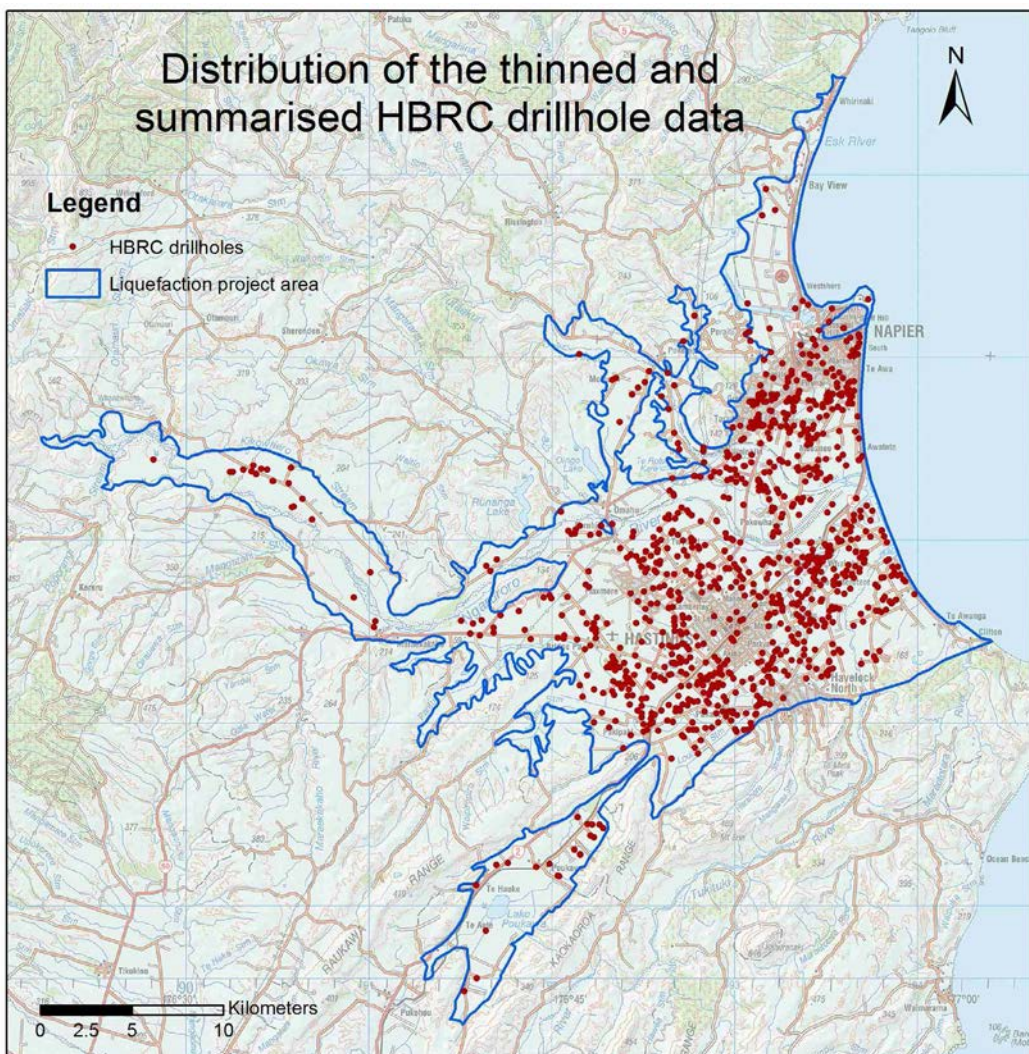


Figure A4.11 Distribution of the thinned boreholes dataset summarised for predominant lithologies at metre by metre intervals down to 10 m depth, and from 10 to15m.

A4.4.5 Summary of Borehole Data

The principal purpose of drilling the boreholes was to locate available groundwater resources, and thus the record of gravels in the logs is relatively good. It is possible to locate the gravel that undoubtedly represents the late Last Glacial alluvial gravel plains, from which most of the groundwater is abstracted. The Last Glacial gravel surface dips NNW beneath the plains from its surface exposure at Havelock North to a maximum depth near the NW side of the plains before rising steeply to the north-western edge of the basin.

Holocene materials overlying this gravel surface show little laterally coherent stratigraphy, with lithologies mostly comprising 'clay' (probably silt and minor clay), silt, sand and gravel. Locally within this volume of Holocene materials some coherent packets of gravel have been modelled close to the major rivers, the Ngaruroro, Tukituki and the Tutaekuri where they feed into the Heretaunga Plains, and to beach barrier bar gravel accumulations in the Marine Parade and Te Awanga areas. The distributions of gravels and fine-grained materials appear to be influenced by active tectonic structures across the Heretaunga Plains, with an absence or relative scarcity of fine grained materials northwest of a line between Bridge Pa and Taradale. Otherwise there is little other discernible pattern of coherent stratigraphy within the fine-grained deposits making up most of the Holocene volume. The three-dimensional distribution of Holocene shells beneath the plains is elongate to the SW, extending all the way to Pakipaki, and indicates the presence of a Holocene embayment (probably estuarine). The north-western shoreline of this embayment extends along a similar line to the active structural boundary referred to above. About 10,000 years ago, the shoreline had penetrated the eastern Heretaunga Plains area between Napier City, Jervoistown and Clive, and by 8000 years ago it had transgressed into central Hastings. The maximum extent of the marine transgression was at c. 7000 years, and the shoreline extended from the western margin of the Ahuriri Estuary through Taradale to Woolwich, Pakipaki, and the north-western edge of Havelock North to Clifton. A gravel barrier bar close to the present-day shoreline had been established at least part way across the embayment from the north by about 8000 years ago.

This lack of continuous horizons within the lithological stratigraphy of Holocene materials contrasts with other coastal locations. In Christchurch, the Wairau Plains, Lower Hutt Valley and the Rangitaiki Plains, the Holocene stratigraphy is consistently represented by a sandy marine incursion across silty and gravelly non-marine deposits and is capped by sandy, silty and gravelly non-marine deposits. Beneath the Heretaunga Plains the only reliable indicator of the Holocene marine incursion and subsequent coastal progradation is derived from the distribution of marine shells. The interaction between fluvial systems and estuarine environments across the Heretaunga Plains, because of tectonic and eustatic sea-level changes through the late Holocene, produced a complex sedimentary environment. This resulted in the lack of clear differentiation in these sediments and the absence of continuous horizons with a consistent depositional origin.

A4.5 REFERENCES

- Barker DHN, Sutherland R, Henrys SA, Bannister SC. 2009. Geometry of the Hikurangi subduction thrust and upper plate, North Island, New Zealand. *Geochemistry Geophysics Geosystems*. 10(2):Q02007. doi:10.1029/2008GC002153
- Beanland S, Melhuish A, Nicol A, Ravens J. 1998. Structure and deformational history of the inner forearc region, Hikurangi subduction margin, New Zealand. *New Zealand Journal of Geology and Geophysics*. 41:325-342.
- Beaven J, Haines J. 2001. Contemporary horizontal velocity and strain rate fields of the Pacific-Australian plate boundary zone through New Zealand. *Journal of Geophysical Research*. 106: 741-770.
- Brackley HL, compiler, Almond P, Barrell DJA, Begg JG, Berryman KR, Christensen S, Dellow GD, Fraser J, Grant H, Harwood N, Irwin M, et al. 2012. Review of liquefaction hazard information in eastern Canterbury, including Christchurch City and parts of Selwyn, Waimakariri and Hurunui Districts. Lower Hutt (NZ): GNS Science. 99 p. +1 CD. (GNS Science consultancy report; 2012/218).
- Brown LJ. 1993. Heretaunga Plains groundwater resource investigations - Flaxmere and Tollemache orchard exploratory water wells. Institute of Geological & Nuclear Sciences client report 732402.11.
- Dravid PN, Brown LJ. 1997. Heretaunga Plains Groundwater Study. Volume 1: Findings. Hawke's Bay Regional Council, Napier. 278 p.
- Griffiths E. 2001. Soils of the Heretaunga Plains: a guide to their management. Havelock North (NZ): Hawke's Bay Regional Council.
- Griffiths E. 1996. Soil map of the Heretaunga Plains. Originally from the Soil map of Heretaunga Plains, Hawke's Bay (DSIR, 1938), and additional surveys from E. Griffiths, G. Smith, B. Purdie, B. McLaughlan (Soil Bureau 1971-1991), and by E Griffiths, 1991-1995.
- Kelsey HM, Hull AG, Cashman SM, Berryman KR, Cashman PH, Trexler JH, Begg JG. 1998. Paleoseismology of an active reverse fault in a forearc setting: the Poukawa fault zone, Hikurangi forearc, New Zealand. *Geological Society of America Bulletin*. 110:1123-1148.
- Lee JM, Townsend DB, Bland KJ, Kamp PJJ, compilers. 2011. Geology of the Hawke's Bay area: [map]. Lower Hutt (NZ): GNS Science 1 map + 86 p, scale 1:250,000. (Institute of Geological & Nuclear Sciences 1:250,000 geological map; 8).
- Lee JM, Tschritter C, Begg JG. 2014 A 3D geological model of the Greater Heretaunga/Ahuriri Groundwater Management Zone, Hawke's Bay. Lower Hutt (NZ): GNS Science. 31 p. (GNS Science consultancy report; 2014/89).
- Ota Y, Berryman KR, Brown LJ, Kashima K. 1989. Holocene sediments and vertical tectonic downwarping near Wairoa, northern Hawkes Bay, New Zealand. *New Zealand Journal of Geology and Geophysics*. 32(3):333-341
- Pillans B, Chappell J, Naish TR. 1998. A review of the Milankovitch climatic beat: template for Plio-Pleistocene sea-level changes and sequence stratigraphy. *Sedimentary Geology*. 122:5-21.
- Rabineau M, Berne S, Olivet J-L, Aslanian D, Guillocheau F, Joseph P. 2006. Paleo sea levels reconsidered from direct observation of paleoshoreline position during Glacial Maxima (for the last 500,000 yr). *Earth and Planetary Science Letters*. 252:119-137.
- Siddall M, Rohling EJ, Almogi-Labin A, Hemleben Ch, Meischner D, Schmelzer I, Smeed DA. 2003. Sea-level fluctuations during the last glacial cycle. *Letters to Nature*. 423:853-858.

- Walcott RI. 1978. Present tectonics and late Cenozoic evolution of New Zealand. *Geophysical Journal of the Royal Astronomical Society*. 52:137-164.
- Wallace LM, Reyners ME, Cochran UA, Bannister SC, Barnes PM, Berryman KR, Downes GL, Eberhart-Phillips D, Fagereng A, Ellis SM, et al. 2009. Characterizing the seismogenic zone of a major plate boundary subduction thrust: Hikurangi Margin. *New Zealand. Geochemistry Geophysics Geosystems*. 10(10):Q10006. doi:10.1029/2009GC002610
- Wilde RH, Ross CW, Dando JL. 2006. Soils of Hastings City and their infiltration rates and permeabilities. Lincoln (NZ): Landcare Research. [Landcare Research Contract Report: LC0607/035 prepared for the Hastings District Council]

A5.0 APPENDIX 5: GEOTECHNICAL DATA, CONE PENETROMETER ANALYSIS, LIQUEFACTION SEVERITY NUMBER AND LAND DAMAGE CORRELATIONS

A5.1 GEOTECHNICAL DATA

An outcome of this project was to develop a geotechnical database containing CPT, SPT, borehole logs and other geotechnical data for the region, which would become a common repository for future geotechnical information. Modifications were made to the Canterbury Geotechnical Database (<https://canterburygeotechnicaldatabase.projectorbit.com/>) so that it could be used as a repository for the data. Tonkin + Taylor (T+T) hosted and provided technical support for the database. It was hoped that local geotechnical consulting firms would see the benefits of sharing geotechnical data and contribute data to the database. However, there was reluctance from the geotechnical community in the Hawkes Bay to share data.

A5.1.1 Development of A Geotechnical Database for Hawke's Bay

CPT data had to be cleaned before it could be analysed (removal of data where two different CPT traces were available for the same site and the correct data could not be determined from existing information). The data was then thinned to remove CPT collar files with no data and CPTs with less than 5 m of data. At about half the sites, the top metre or so was untested as sites required hand-dug 'pre-drill' pits to ensure no shallow buried infrastructure would be punctured. This leaves a gap in the geotechnical models between the surface and about 1 m depth for these sites. There was no pre-drill information for the RDCL CPT data.

A5.2 CPT ANALYSIS

Liquefaction Severity Numbers (LSNs) were calculated for each CPT using the parameters given above. LSN is a calculated liquefaction hazard parameter developed by T+T (2013) using the Canterbury Earthquake damage dataset of >7000 CPTs, 1000 boreholes and 800 groundwater monitoring wells in the Christchurch area. It was designed to reflect the more damaging effects of shallow liquefaction on residential land and foundations, specifically in Christchurch, where results could be checked against the actual distribution and severity of liquefaction during specific earthquakes. LSN considers depth weighted volumetric densification strain within soil layers as a proxy for the severity of liquefaction land damage likely at the surface (T+T, 2013). LSN is defined as:

$$LSN = 1000 \int \frac{\varepsilon_v}{z} dz$$

where ε_v is the calculated post-liquefaction volumetric reconsolidation strain entered as a decimal, and z is the depth below the ground surface in metres for depths greater than 0.0 m. In practice, LSN is calculated as the summation of the post-liquefaction volumetric reconsolidation strains, each calculated for an underlying soil layer divided by the depth to the midpoint of that layer. Further details about LSN and its derivation and testing can be found in T+T (2013).

The LSN parameter best correlates with the likelihood of vertical differential ground surface subsidence occurring away from lateral spread areas (i.e., rivers and streams), and is a better estimate for the prediction of flat land liquefaction damage (i.e., sand boils and differential ground surface settlement) than other liquefaction damage prediction methods (e.g.,

Liquefaction Potential Index or LPI). It is the vertical differential ground surface subsidence that causes the structural deformation to residential houses.

Unfortunately, none of the parameters above are suitable for predicting the amount of horizontal movement, or lateral spreading. However, the S_{V1D} parameter can be used as a proxy to estimate the maximum extents of the horizontal movement due to lateral spreading. Generally, once the maximum extents of lateral spreading are estimated, the maximum amount of horizontal movement will occur next to the river and decay with distance away from the river. For loss modelling purposes, a linear decay model was developed.

The total horizontal movements at the river banks were estimated based on the observations from Christchurch. In Christchurch, it was observed that the maximum horizontal movement was generally in the order of 0.5 to 2 m. It was also observed that the maximum movement was roughly proportional to the extent of land involved in lateral spreading (i.e., small areas of land which were involved in spreading did not have the same severity of lateral spreading near the river banks compared to large areas of land which were involved in spreading). Therefore, for loss modelling purposes a simplifying assumption was made that the amount of horizontal displacement at the river edge is proportional to the extent of lateral spreading (i.e., 2 m at the river edge when the maximum extent is 200 m, reducing to 0.5 m at the river edge when the maximum extent is 25 m).

The extent of lateral spreading was estimated using the post-liquefaction reconsolidation settlement index (S_{V1D}) and the river depth. The S_{V1D} value is a measure of the thickness of the water film which is expected to develop in the soil and is a better representation of lateral spreading than that provided by LSN (van Ballegooij et al., 2015). The S_{V1D} parameter is defined as:

$$S_{V1D} = \int \varepsilon_v dz$$

where ε_v is the calculated volumetric strain and z is the depth to the layer of interest (van Ballegooij et al., 2015).

S_{V1D} can be used a proxy threshold for determining, on a portfolio basis, whether lateral spreading is likely to occur at a particular distance from the river bank. The greater the distance from the river, the higher the calculated S_{V1D} needs to be to produce lateral spreading. For example, if the calculated S_{V1D} is 105 mm for a particular level of earthquake shaking, then lateral spreading next to the lower reaches of the main rivers is predicted to occur up to 100 m back from the river bank. The values of S_{V1D} and distance from the river bank, and corresponding LSN values used as proxies for predicting the extent of lateral spreading for main-stem rivers (such as the lower reaches of the Avon River in Christchurch), which are typically 3 to 5 m depth, are shown in Table A5.1. The corresponding values for S_{V1D} and LSN for smaller tributary streams, typically 2 to 3 m deep, are shown in Table A5.2. More detail on S_{V1D} and its derivation can be found in van Ballegooij et al. (2015).

Table A5.1 Proxy S_{V1D} and LSN values for various distances from the top of the river bank for main stem channels (typically, 3–5 m deep).

Distance from the river bank	S_{V1D}	LSN
0 to 25m	>25	>7
25 to 50m	>50	>15
50 to 100m	>75	>20
100 to 150m	>150	>25
150 to 200m	>200	>30

Table A5.2 Proxy SV1D and LSN values for various distances from the top of the river bank for tributary channels and the lower (downstream) reaches of main-stem channels (typically, 2–3 m deep).

Distance from the river bank	SV1D	LSN
0 to 10m	>25	>7
10 to 25m	>50	>15
25 to 50m	>100	>20
50 to 100m	>200	>30

The SV1D parameter better correlates with the total vertical ground surface subsidence away from lateral spread areas (than LSN). When subsidence due to liquefaction occurs in low lying areas the land and houses can become more flood prone. It is the total vertical ground surface subsidence that causes this type of secondary damage.

Using SV1D values was preferred as a proxy for predicting lateral spreading over LSNs for the following three reasons:

1. SV1D values have better physical meaning and relationship to lateral spreading compared to using LSN values; and
2. The SV1D proxy thresholds have been applied in Christchurch and at a portfolio level they have proven to work well in identifying the general locations and amount of properties predicted to be affected by lateral spreading when compared against the Canterbury Earthquake Sequence (CES) observations.
3. The LSN proxy thresholds have not yet been applied in Christchurch to check that they appropriately identify the general locations and number of properties predicted to be affected by lateral spreading when compared against the CES observations.

A5.3 LAND AND BUILDING DAMAGE CORRELATION WITH LSN

Liquefaction related land damage mapping of residential properties in Canterbury was carried out immediately after the September 2010, February 2011, and June 2011 earthquakes to assess the extent and severity of the surface effects of liquefaction. The mapping was supplemented by interpretation of aerial photography after each of the four main earthquakes to identify areas where liquefaction ejecta occurred, but which may have been cleaned up by the time the ground teams arrived to map the areas.

These ground and aerial land damage observations, as well as information collected during subsequent detailed property assessments, were combined to produce standardised land damage observation maps after each of the four main earthquakes. These maps categorised the observed land damage into three categories:

- **None-to-minor** – no observed liquefaction related land damage through to minor observed ground cracking but with no observed ejected liquefied material at the ground surface;
- **Minor-to-moderate** – observed ground surface undulation and minor-to-moderate quantities of observed ejected liquefied material at the ground surface but with no observed lateral spreading; and
- **Moderate-to-severe** – large quantities of observed ejected liquefied material at the ground surface and severe ground surface undulation and/or moderate-to-severe lateral spreading.

The mapped liquefaction related land damage for each of the events is shown in Figure A5.1.

The predicted land performance based on the 2010 to 2011 Canterbury Earthquake Sequence (CES) earthquakes was assessed by calculating event specific LSN values for each property using the estimated PGA and groundwater levels for the September 2010, February 2011 and June 2011 earthquake events. The LSN value for each property was then correlated with the corresponding observed land damage for each respective event.

The correlations showed that the frequency distribution of calculated LSN for each land damage observation grouping was relatively consistent with the correlations for each of the three earthquake events. These datasets were combined and box plots and histograms of the data are shown in Figure A5.2.

The plots on Figure A5.2 show that an LSN value of less than 16 characterises properties with none-to-minor liquefaction related land damage and some minor-to-moderate liquefaction related land damage. Whereas an LSN value of greater than 16 characterises properties with moderate-to-severe liquefaction related land damage and some properties with minor-to-moderate liquefaction related land damage.

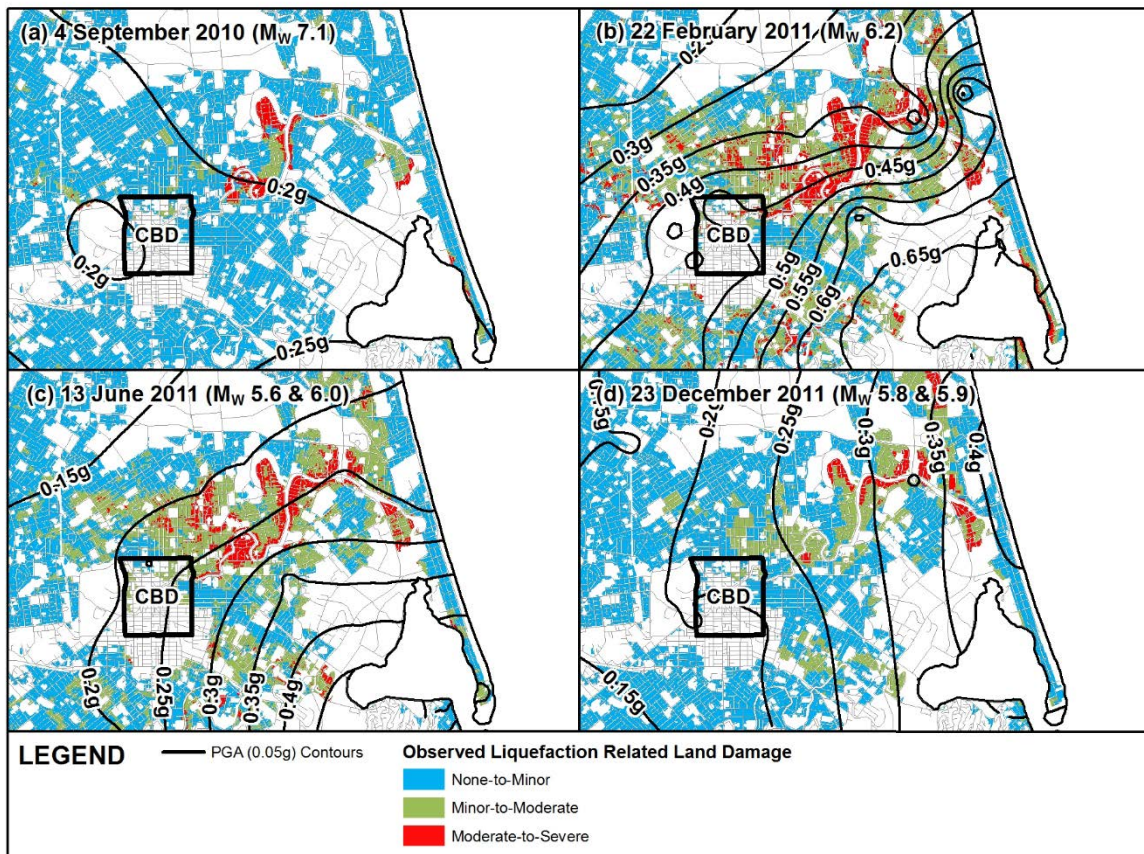


Figure A5.1 Map showing the inferred levels of earthquake shaking and the observed land damage for urban residential properties in Christchurch after the (a) 4 September 2010, (b) 22 February 2011, (c) 13 June 2011 and (d) 23 December 2011 earthquakes.

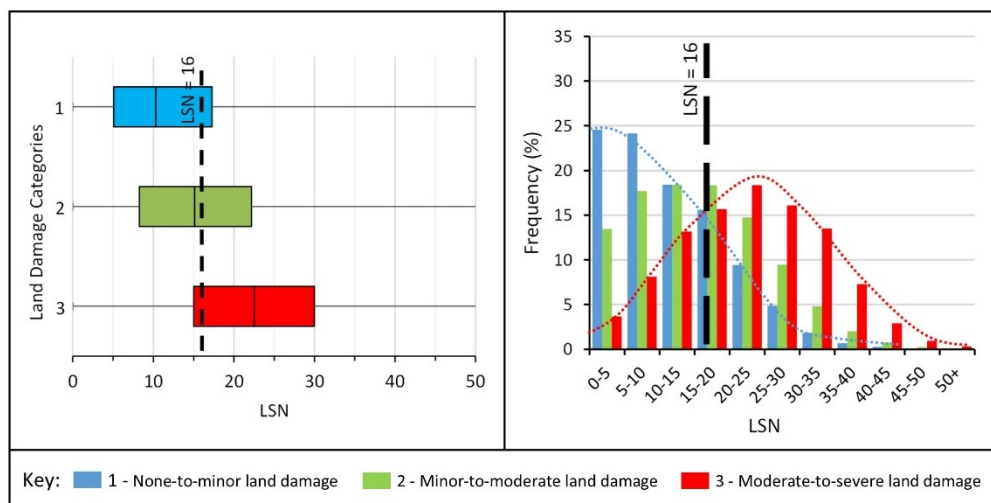


Figure A5.2 (a) Box and whisker plot showing the distribution of land damage observations correlated against LSN for the 4 September 2010, 22 February 2011 and 13 June 2011 earthquake events (b) histogram showing the distribution of land damage observations correlated against LSN.

Figure A5.3 shows the likelihood of the liquefaction related damage for different banding of LSN. For high calculated LSN values the likelihood of moderate-to-severe liquefaction related land damage is very high and the likelihood of none-to-minor liquefaction related land damage is very low. Conversely, for low calculated LSN values the likelihood of moderate-to-severe liquefaction related land damage is very low and the likelihood of none-to-minor liquefaction related land damage is very high.

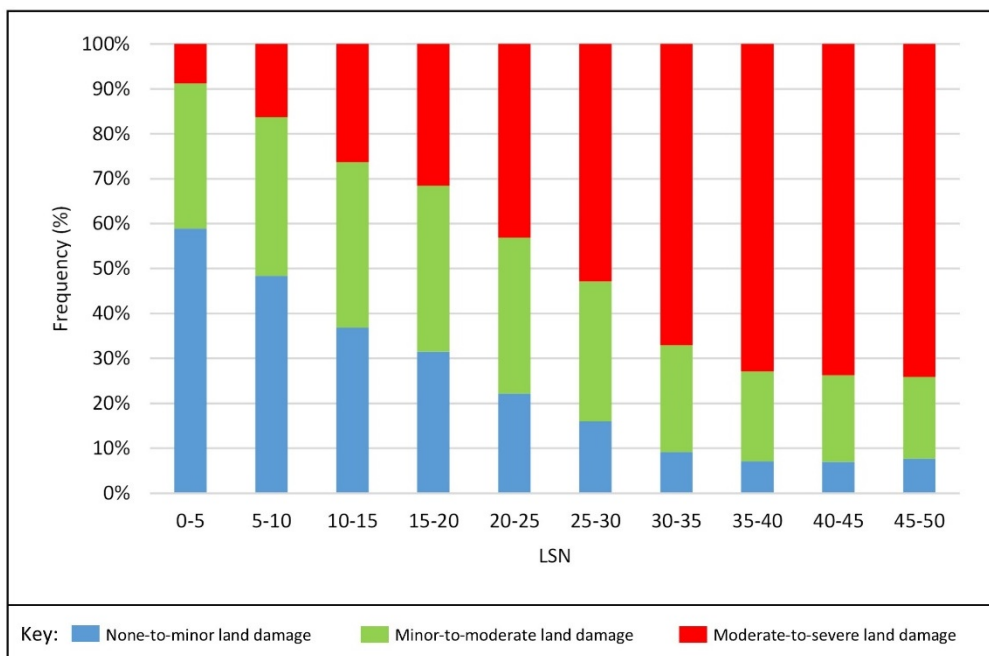


Figure A5.3 Frequency bar chart showing the likelihood of none-to-minor, minor-to-moderate, and moderate-to-severe land damage for different LSN bands.

Liquefaction of near surface soil layers (mainly in the upper 10m of the soil profile) had the following effects:

- Volumetric densification;
- Sand and water ejecta;
- Topographic re-leveelling; and
- Lateral spreading.

These effects resulted in differential ground surface subsidence. When this differential ground surface subsidence occurred beneath residential buildings founded on shallow foundation systems, it resulted in differential settlement of the foundations (Chapman et al. 2015).

Figure A5.4 (a) shows the estimated differential foundation settlement of residential dwellings in Christchurch based on sixty thousand visual inspections. It is important to note that because these estimations of differential foundation settlement were based on a visual inspection they are inherently subjective. Furthermore, this estimate of differential foundation settlement is different from angular distortion. Angular distortion is a measurement of the gradient of the slope over part or all of the building foundation and is independent of the length of the building.

The information was collected as part of a detailed inspection of liquefaction related land damage for EQC land damage claim assessment purposes. The inspections were carried out by the Land Damage Assessment Team (LDAT) which included approximately 400 geotechnical engineers and engineering geologists. The inspections were predominantly focused in the areas affected by liquefaction land damage.

The visual estimate of differential settlement to residential building foundations was recorded based on criteria reflecting its severity. The data for each residential house was collected to identify three categories of differential settlement, which were described on the assessment forms as:

- **None/minor** – less than 20 mm;
- **Moderate** – 20 to 50 mm; and
- **Major** – greater than 50 mm.

Sixteen thousand residential buildings were assessed as having major (> 50 mm) differential settlement. Comparison with Figure A5.1 shows that this assessment is closely correlated with the properties that have moderate-to-severe mapped land damage.

Figure A5.4 (b) shows the Building Damage Ratio (BDR) values of the portfolio of residential buildings in the Christchurch area. The BDR is calculated by dividing the cost to repair earthquake related damage to a residential building by the value of that building. The building damage repair costs were assessed by an independent team to the LDAT assessment team.

When the BDR of a residential building is greater than 0.5, the damage to that building is typically significant. This damage often results from liquefaction related foundation deformation which is impractical to repair. In many cases this results in the building being rebuilt because the cost of repair exceeds the cost of rebuilding.

BDR values between 0.3 and 0.5 typically represent practical repairable damage such as cosmetic repairs and minor structural repairs. Often this also includes minor foundation re-levelling of the building. BDR values of less than 0.3 generally comprise only non-structural damage such as repairing cracks in the internal wall plaster lining and repainting the house. Typically, this does not involve foundation repair works.

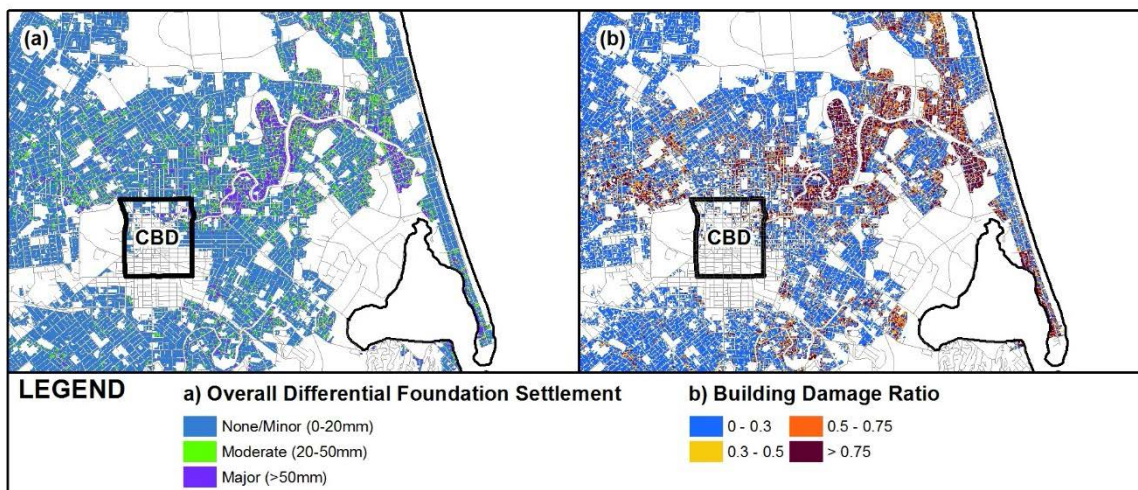


Figure A5.4 (a) Estimated differential foundation settlement from visual inspections of the urban residential buildings in Christchurch as a result of the CES and (b) the associated BDR.

Comparison with Figure A5.1 shows that properties with BDR of greater than 0.5 are closely correlated with the properties that have moderate-to-severe mapped land damage.

Similar liquefaction analyses (as undertaken for the mapped land damage (described above) have been undertaken for the residential buildings in the TC3 and residential Red Zone areas in Christchurch for two groups of differential foundation settlement (less than and greater than 50 mm) and three groups of BDR (less than 0.3, between 0.3 and 0.5 and greater than 0.5). The results from these analyses are shown in Figure A5.5 and Figure A5.6 respectively.

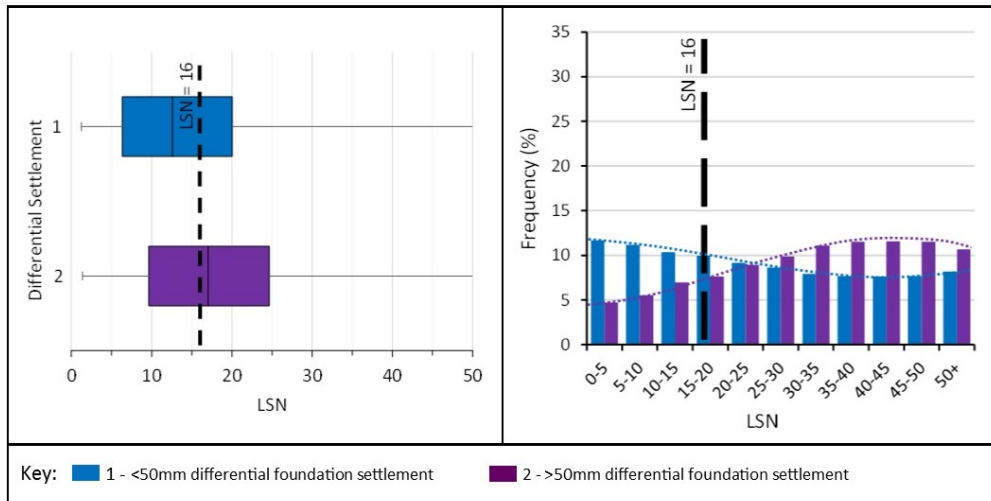


Figure A5.5 (a) Box and whisker plot showing the distribution of differential foundation settlement for residential dwellings in the TC3 and residential Red Zone areas correlated against LSN for the September 2010, February 2011 and June 2011 earthquake events (b) histogram showing the distribution of differential foundation settlement correlated against LSN.

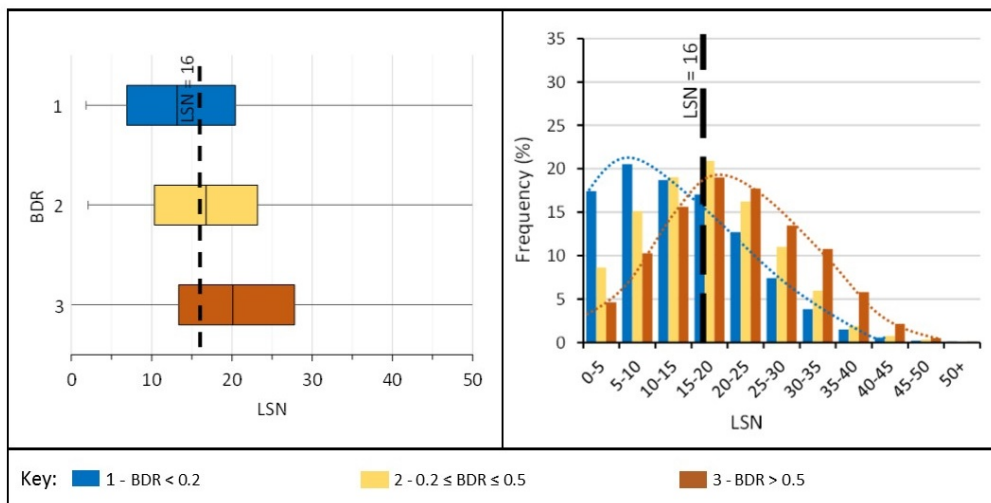


Figure A5.6 (a) Box and whisker plot showing the distribution of BDR for the residential dwellings in the TC3 and residential Red Zone areas correlated against LSN for the September 2010, February 2011 and June 2011 earthquake events (b) histogram showing the distribution of BDR correlated against LSN.

Figure A5.5 shows that the distribution of differential foundation settlement for properties with LSN values greater than 16 is higher than the distribution of differential foundation settlement properties with LSN values of less than 16. It is important to recognise that a certain level of total and differential settlement is already typically allowed for in the design of buildings.

The reason the correlation of LSN with differential settlement is not as well separated for the two populations of properties is under consideration (i.e., < 50 mm and > 50 mm differential foundation settlement). The main reasons for why the two populations are not well separated are:

- The differential foundation settlement data were obtained by visual assessment;
- Some buildings with moderate-to-severe land damage did not settle differentially;
- Some building construction types and shapes are more rigid than others and therefore are more resistant to differential settlement; and

- Differential foundation settlement is not the ideal measure of building deformation because 50 mm of differential settlement is more likely to occur over a larger building footprint than 50 mm of differential settlement over a smaller building footprint. Angular distortion is a better indicator of foundation deformation and would probably provide a better correlation with LSN.

Similar to the land damage correlations (shown in Figure A5.1), Figure A5.6 shows that the LSN values greater than 16 characterise properties with a distribution of higher BDR values whereas LSN values of less than 16 characterise properties with a distribution of lower BDR values. It is noted that these properties were all subject to similar levels of earthquake shaking and therefore the distribution of higher BDR values at LSN values greater than 16 provides clear evidence that liquefaction is having a material consequence on the damage of the residential dwellings.

Figure A5.5 and Figure A5.6 show how the likelihood of differential foundation settlement and BDR respectively change for different banding of LSN. For high calculated LSN values the likelihood of buildings with high BDR is high and the likelihood of buildings with low BDR is low. Conversely, for low calculated LSN values the likelihood of buildings with high BDR is low and the likelihood of buildings with low BDR is high.

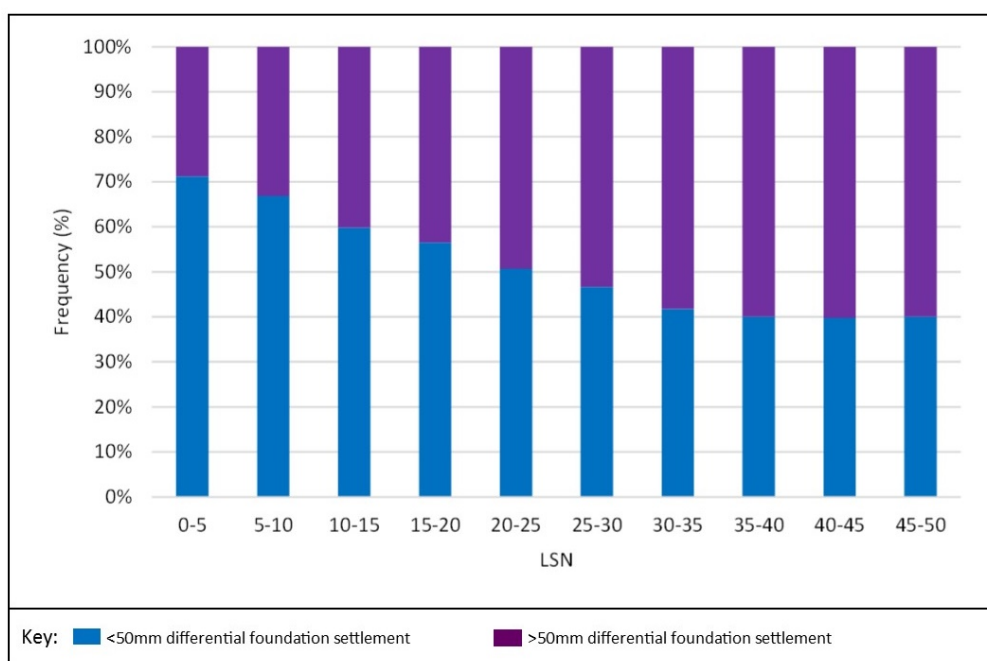


Figure A5.7 Frequency bar chart showing the likelihood of differential foundation settlement of less than and greater than 50mm for different LSN bands.

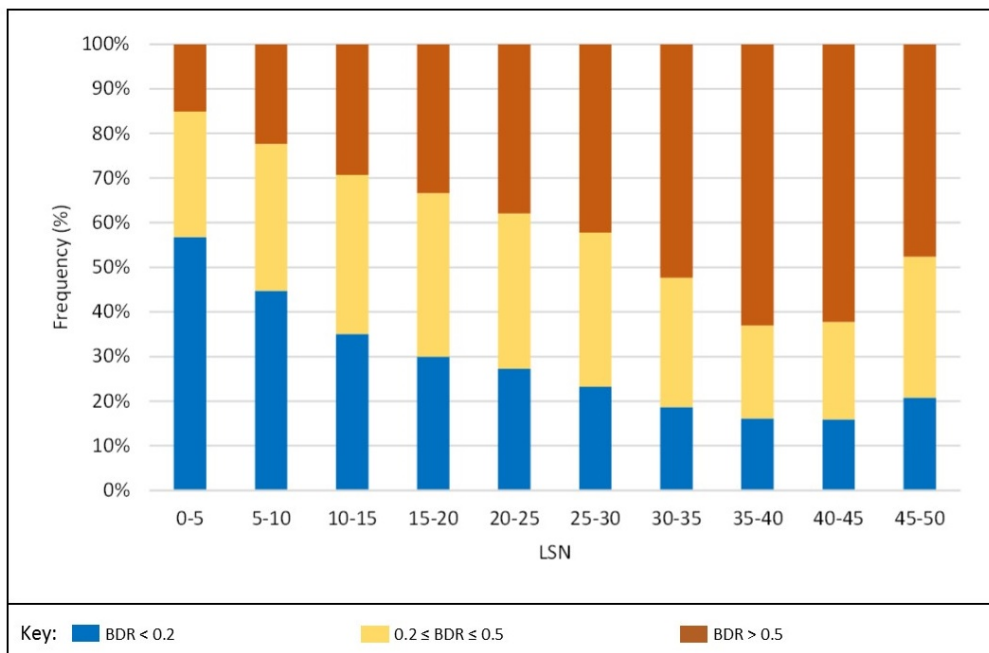


Figure A5.8 Frequency bar chart showing the likelihood of BDR values of less than 0.3, 0.3 to 0.5 and greater than 0.5 for different LSN bands.

A5.4 ACRONYMS

Ground motions

PGA	Peak ground acceleration
M	Magnitude

General

CGD	Canterbury Geotech Database
CPT	Cone penetration test

CPT, soil and liquefaction triggering parameter

q_c	CPT tip resistance
I_c	CPT inferred soil behaviour index type
I_c cut-off	The threshold above which the soil is considered too clay-like in behaviour to liquefy
FC	Soil fines content (i.e., the percentage by weight less than 75 micron)
C_{FC}	A fitting parameter used in a correlation between FC and I_c
P_L	Probability relating to the uncertainty of the liquefaction triggering methods

Liquefaction Vulnerability Parameters – calculated from CPT

LSN	Liquefaction severity number
S_{V1D}	Volumetric one dimensional consolidation settlement

A5.5 REFERENCES

- Chapman L, van Ballegooy S, Ashby G, Lacrosse V, Burgess S. 2015. Correlation of differential building settlement with predicted CPT-based liquefaction vulnerability parameters. Christchurch, New Zealand, ISSMGE.
- Tonkin & Taylor. 2013. Liquefaction vulnerability study. Report to Earthquake Commission. Tonkin & Taylor Ltd. (T&T report; 52020.0200/v1.0). February 2013.
- van Ballegooy S, Green RA, Lees J, Wentz R, Maurer BW. 2015. Assessment of various CPT based liquefaction severity index frameworks relative to the Ishihara (1985) H1-H2 boundary curves. Submitted to SDEE, Special Issue: Liquefaction in NZ/Japan. August 2015.

A6.0 APPENDIX 6: GROUNDWATER SURFACE MODELLING

Depth to the unconfined groundwater surface (UGS) is a critical factor in determining liquefaction susceptibility, because liquefaction can occur only when materials of suitable grain-size distributions are saturated. This section describes the data and methodology used to model a surface representing this UGS, with some comparisons made to a recent UGS model created for the Christchurch region (van Ballegooij et al., 2013). Due to the large area covered, the UGS was calculated within three different zones (Figure A6.1).

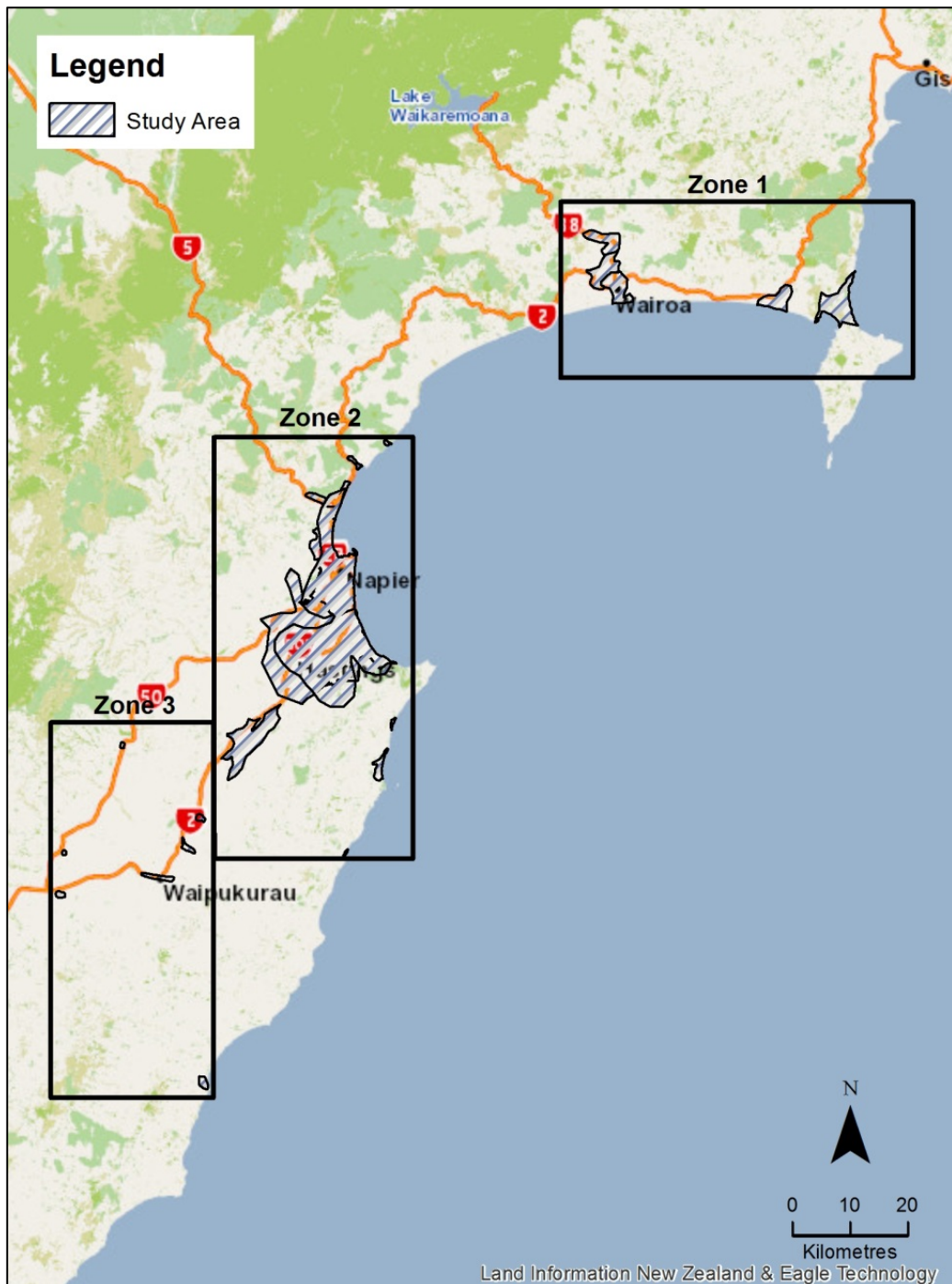


Figure A6.1 Three zones used for developing the unconfined groundwater surface.

A6.1 WATER LEVEL DATA

For the Christchurch study (van Ballegooij et al., 2013), the median groundwater surface model was constructed using only time series water level data. To be included in the analysis, the time series was to cover at least 9 months, or have sufficient time series data that the time series could be synthetically projected to cover 9 months.

Within the Hawke's Bay region, the majority of data pertains to confined aquifers. Of the time series data available, only 15 wells within the modelled region are considered to sample the unconfined water table. The median water table level was calculated at these locations using the available data, with sampling periods ranging from 3–22 years. The exact time period used varies for each data set to ensure no bias is induced by seasonal variability. As water level measurements are taken when there is a change in level, the median calculated is for the entire time period rather than the sample set (e.g., Figure A6.2).

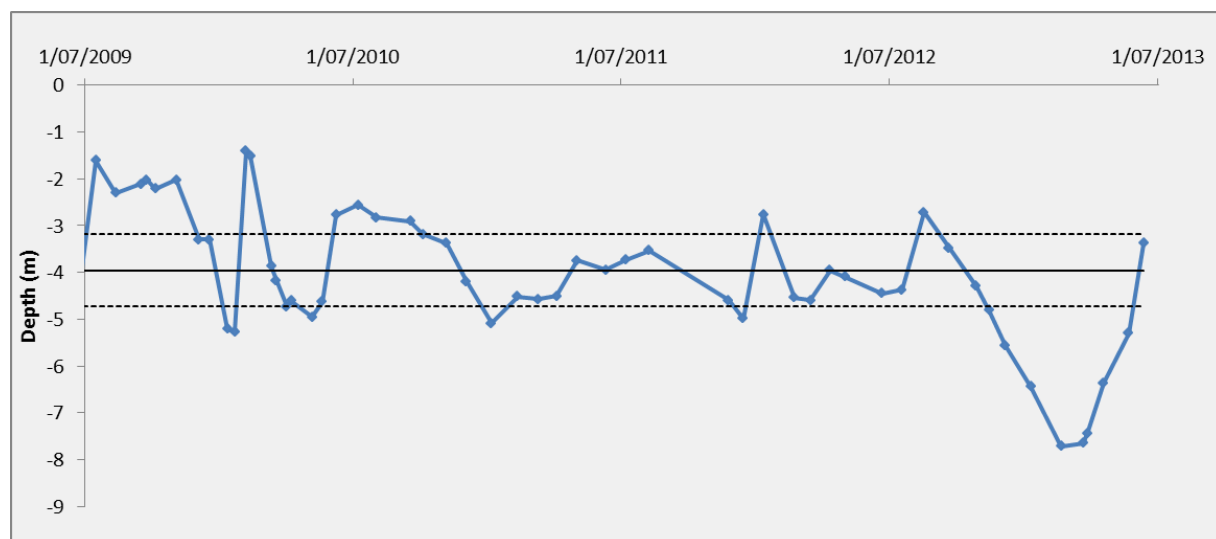


Figure A6.2 Monitoring well no. 1003. The solid black line displays the median water level -3.96 m; the dashed lines display the envelope of the median absolute deviation (mad) of 0.78 m.

As the available time series measurements constitute such a small sample set, static water levels were also used to estimate the water table depth. Uncertainty arises from the use of static water levels for a number of reasons: a single measurement is taken at one point in time; as measurements are usually taken following drilling and development of a groundwater well, it is not always clear from the data whether the well was allowed sufficient time to reach equilibrium (if taken too soon following pumping then the water table depth will be overestimated); it is not always clear from the driller's notes whether the water level measured is from a confined or unconfined aquifer, and this can also be wrongly recorded.

Wells in the HBRC drillhole database were classified according to whether they sampled the unconfined water table or a confined aquifer by interrogation of driller's notes and borehole logs. After datum adjustment to above mean sea level (amsl), any static water levels within the Heretaunga Plains deeper than -1 amsl were removed, as these were considered to be measurements taken during pumping (if the water table was below msl then there would be no flux to the sea). This reduced the original well data set of 7503 down to 449 wells. An additional set of 12 static water level measurements were added from a November 2008 GNS Science survey of the Poukawa aquifer water levels (Cameron, 2011).

During the course of the project, the above data sets were supplemented by 24 new shallow groundwater monitoring wells that were drilled by NCC for this project in early 2014. The available time series water levels from these wells (five data points between March and October 2014) were used to derive median groundwater levels at these locations. Depth to water table estimates from CPT data were also used as static water level measurements.

Time series data from 25 river monitoring sites were provided by Hawke's Bay Regional Council. However, the disparity between river level measurements and the DEM elevations for the corresponding locations were too large to integrate this data. The DEM used is as described in Appendix A4.2.

Mapped surface water features from the New Zealand Topo250 maps (Land Information New Zealand, 2014) were incorporated as data points into the modelling. Due to the comparative scarcity of well data compared to mapped surface water, surface water information sampled from wells tended to bias the results too much towards a very shallow (coincident with ground level) water table. To overcome this, linear surface water features were sampled every 20 km, and polygon surface water features were sampled as a single point in the centre of the feature.

A map of all data used is displayed in Figure A6.3.

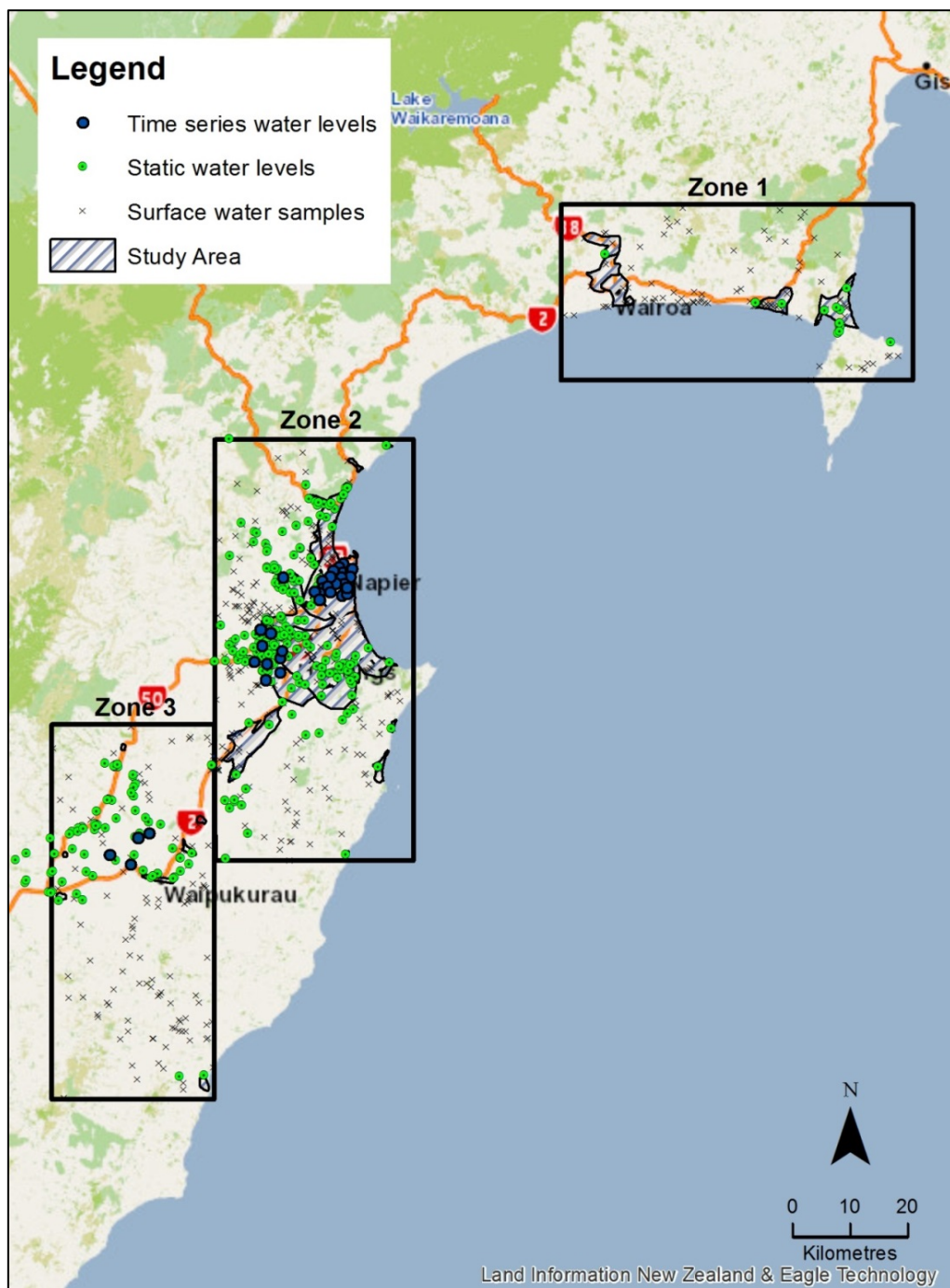


Figure A6.3 All data used to develop the unconfined groundwater surface.

A6.2 INTERPOLATION METHOD

The software Surfer 11.0 was used for data interpolation. van Ballegooij et al. (2013) used the Kriging method for interpolation of the Christchurch median unconfined groundwater surface and identified three preferential interpolation methods that allow for breaklines to model rivers and the coastline, and are suitable for irregularly spaced data: Kriging; Radial Basis function; and Local Polynomial. Following testing of the three methods, the Kriging method was used with a linear drift, search area of 10km, and a Gaussian variogram. The grid size used was 250 m and the coastline and major rivers were set as breaklines at ground level.

Interpolation was performed in metres below ground level (mBGL) and the UGS clipped to both the study area and the extent of mapped Quaternary geology as described by QMAP (Heron et al., 2012). Maps of the UGS in mBGL for three zones are displayed in Figure A6.4 – Figure A6.8, where the shallowest levels are shown by the dark blue and the deepest levels by the dark brown.

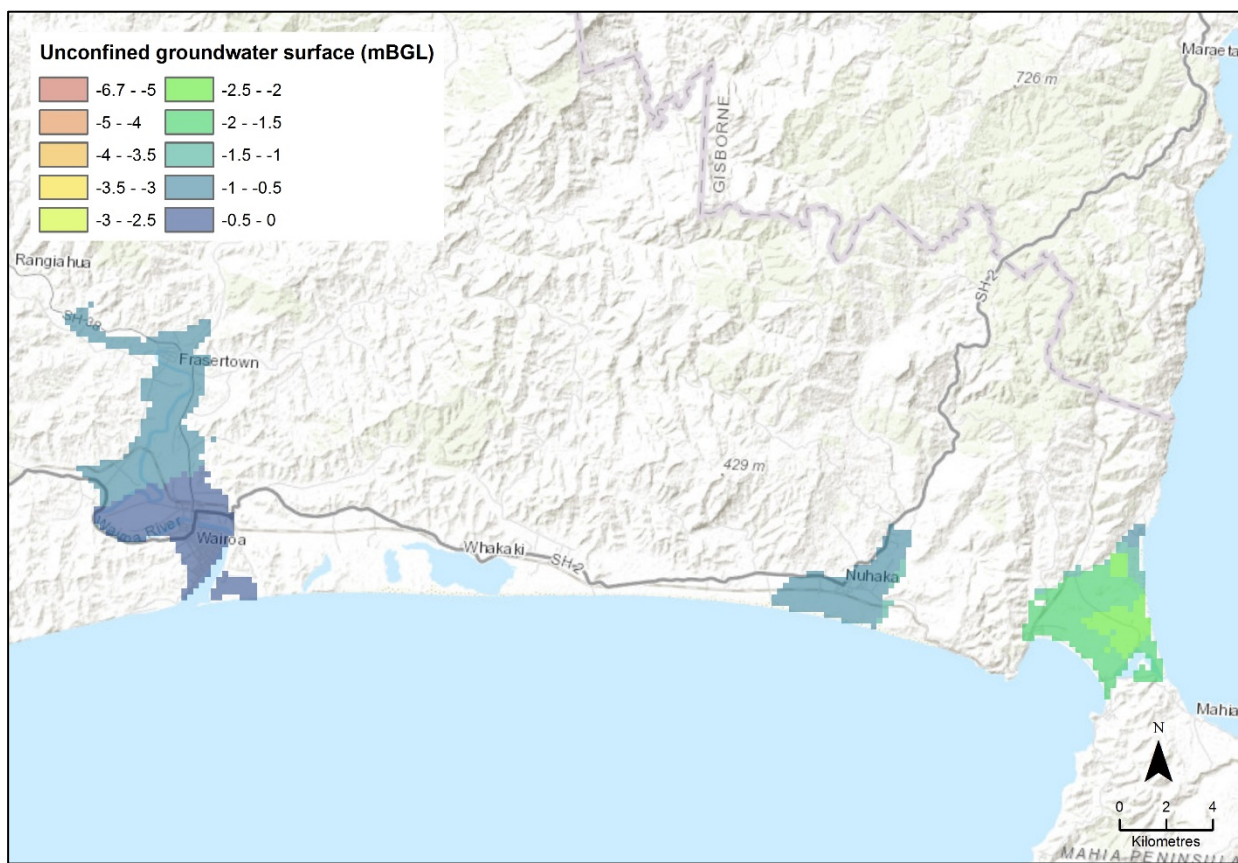


Figure A6.4 Unconfined groundwater surface for Zone 1.

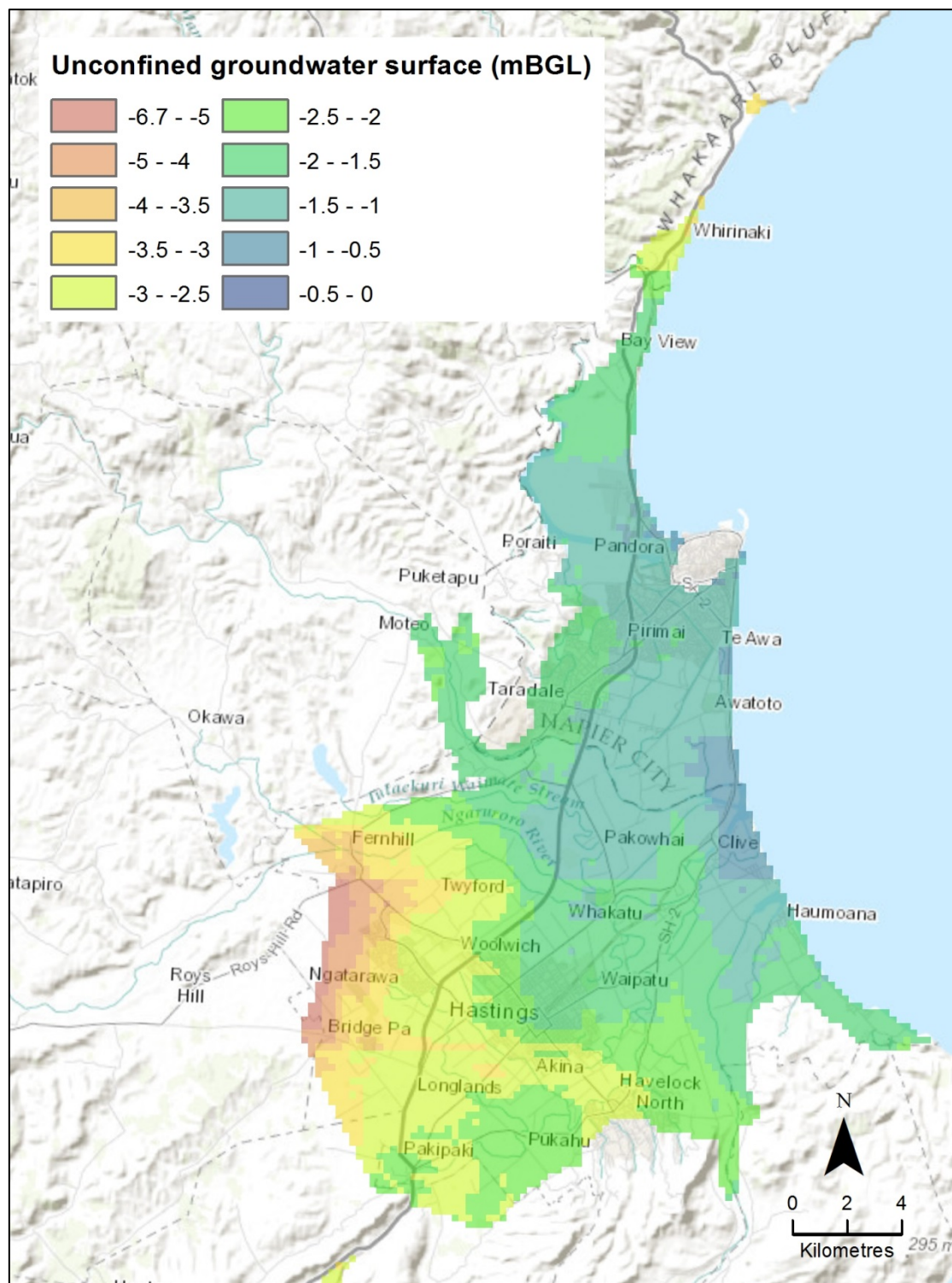


Figure A6.5 Unconfined groundwater surface for the northern portion of Zone 2.

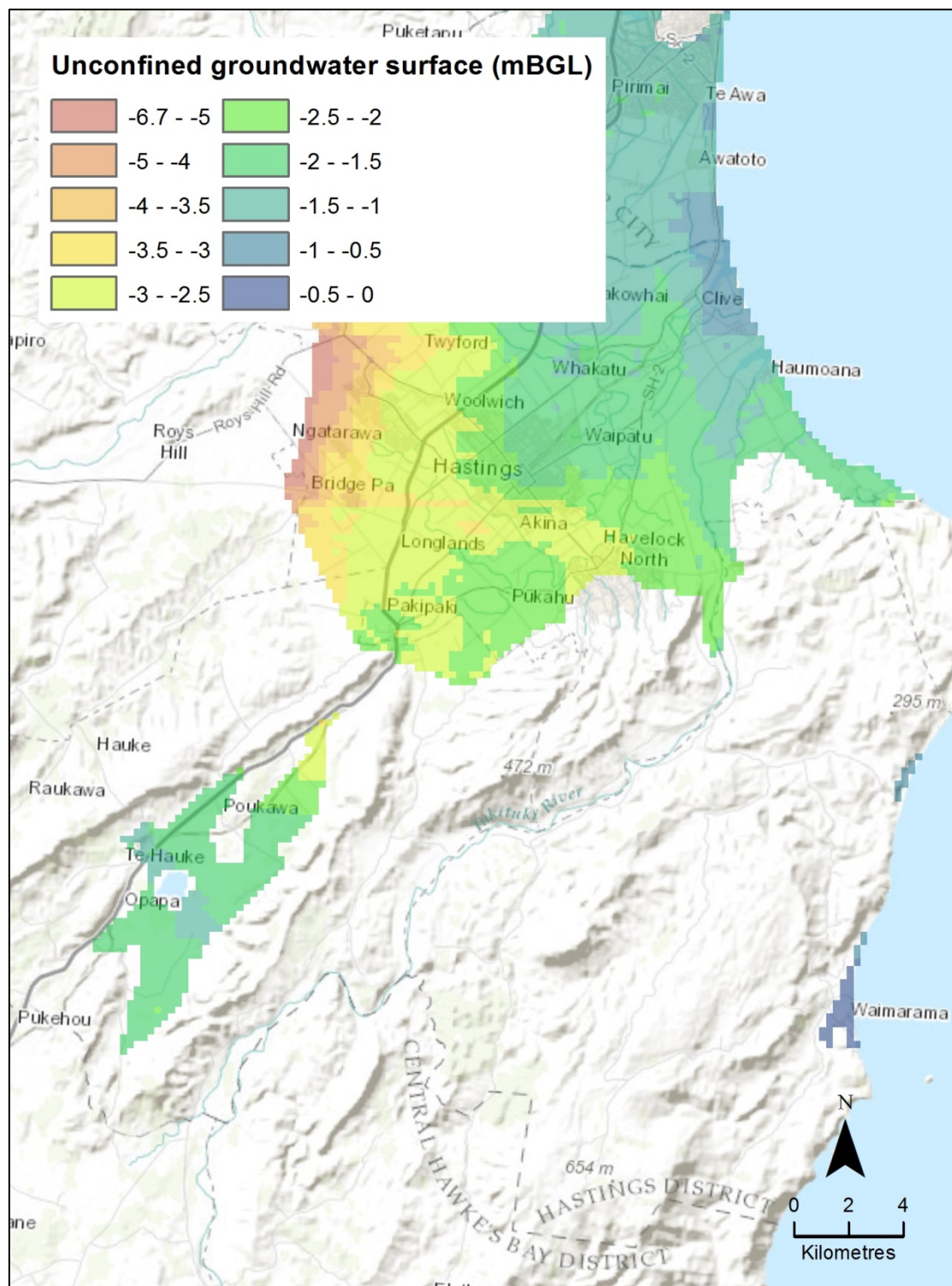


Figure A6.6 Unconfined groundwater surface for the southern portion of Zone 2.

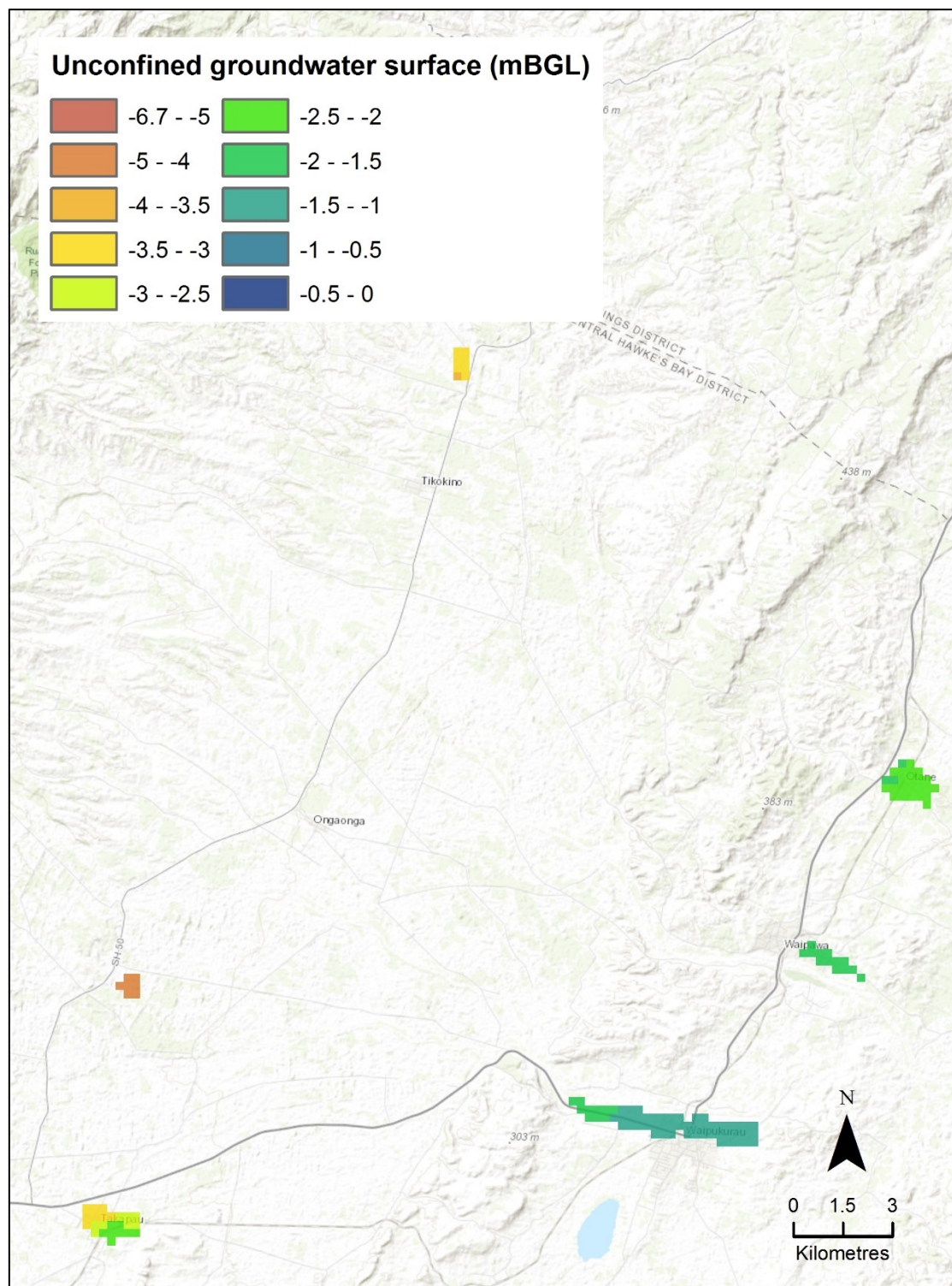


Figure A6.7 Unconfined groundwater surface for the northern portion of Zone 3.

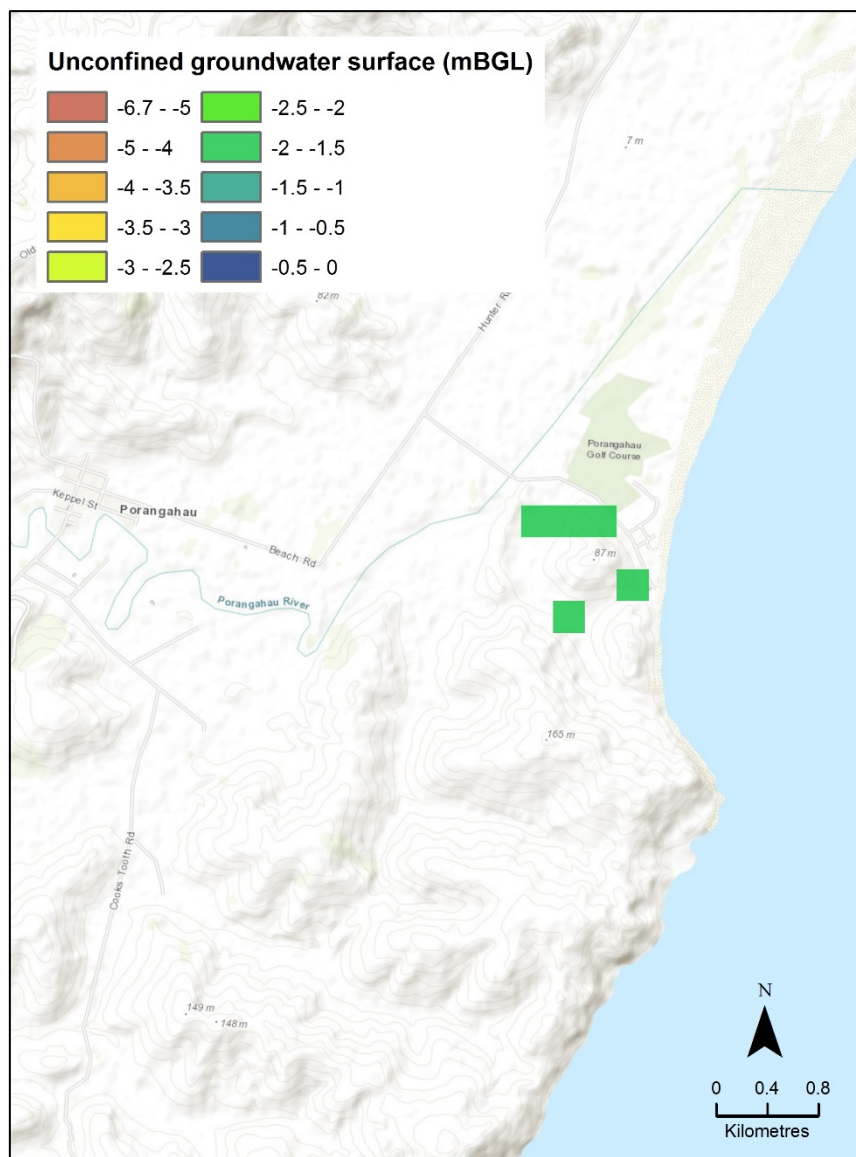


Figure A6.8 Unconfined groundwater surface for the southern portion of Zone 3.

A6.3 UNCERTAINTY

For the time series data used, median absolute deviations (MAD) were calculated. MAD are more robust than standard deviations to extreme values, which vary between 0.05–0.78 m. Of these time series data, seven wells also had associated static water level measurements. The differences between these static water levels and the median levels were calculated, with these differences having a standard deviation of 1.5 m (using the standard deviation rather than the MAD so that any extreme deviations are encompassed in this measurement). This measure of variability is similar to the Summer-Winter variation of 1.5–2.5 m described in the 1997 Heretaunga Plains Groundwater study (Dravid & Brown, 1997). To produce a map of uncertainty, a point density was calculated to produce a map of the measurement density per km. The static water level uncertainty of 1.5 m was classified as the standard measurement uncertainty and was assigned a value of one measurement within the density calculation. Time series measurements have then been weighted based on their MAD values ($w=1.5/\text{MAD}$), such that a MAD of 0.78 m is assigned as 1.9 standard measurements and a MAD of 0.5 is assigned as 3 standard measurements. Mapped surface water features have been down-weighted to 0.33 that of a static water level measurement.

Maps of measurement uncertainty for three zones are displayed in Figure A6.9 – Figure A6.12, where the highest uncertainty is in the red regions, which have low measurement densities, and the lowest uncertainty is in the dark blue regions, which have high measurement densities.

There are a number of regions that are very uncertain: the whole of Zone 1 – especially Wairoa Valley, and to a lesser extent the Mahia sand aquifer; and the small coastal towns.

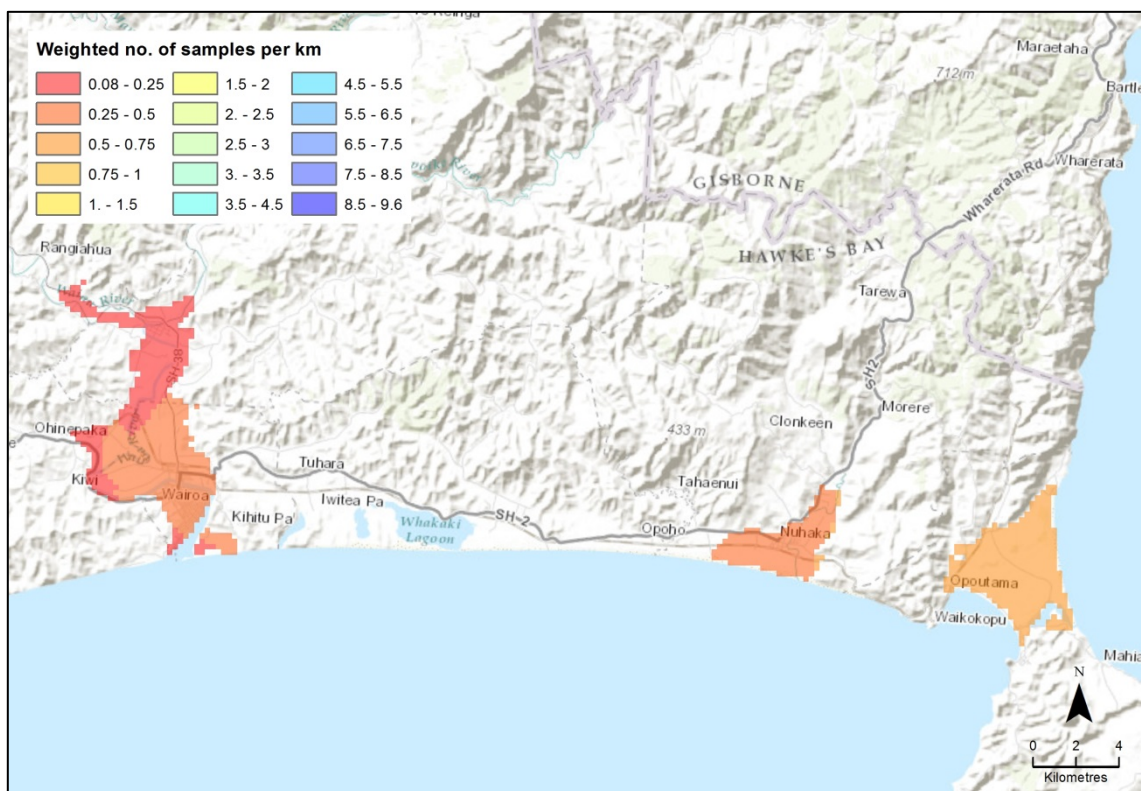


Figure A6.9 Uncertainty map for Zone 1, Wairoa, based on data point density as described in the text.

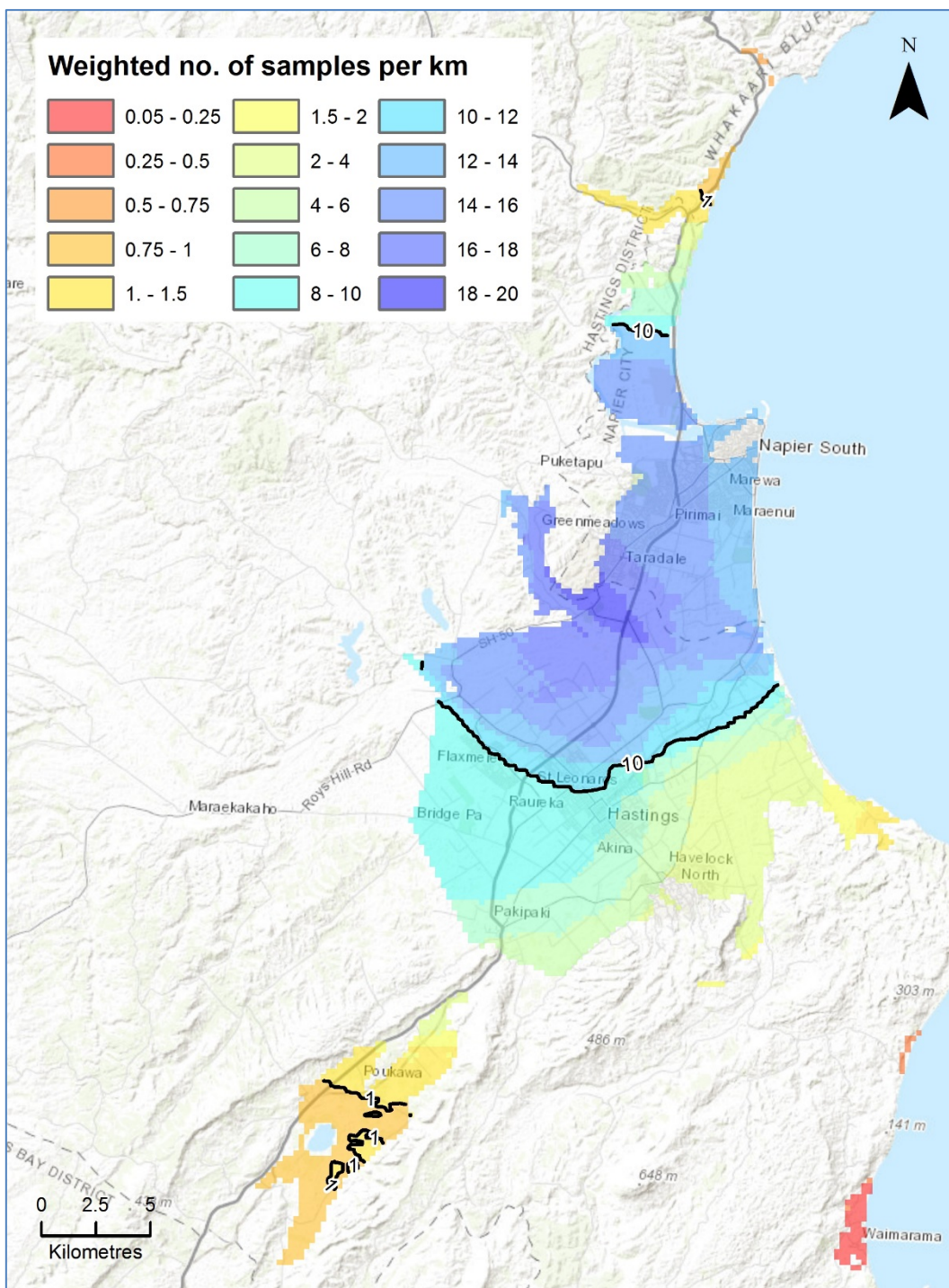


Figure A6.10 Uncertainty map for Zone 2, the Heretaunga Plains, based on data point density as described in the text.

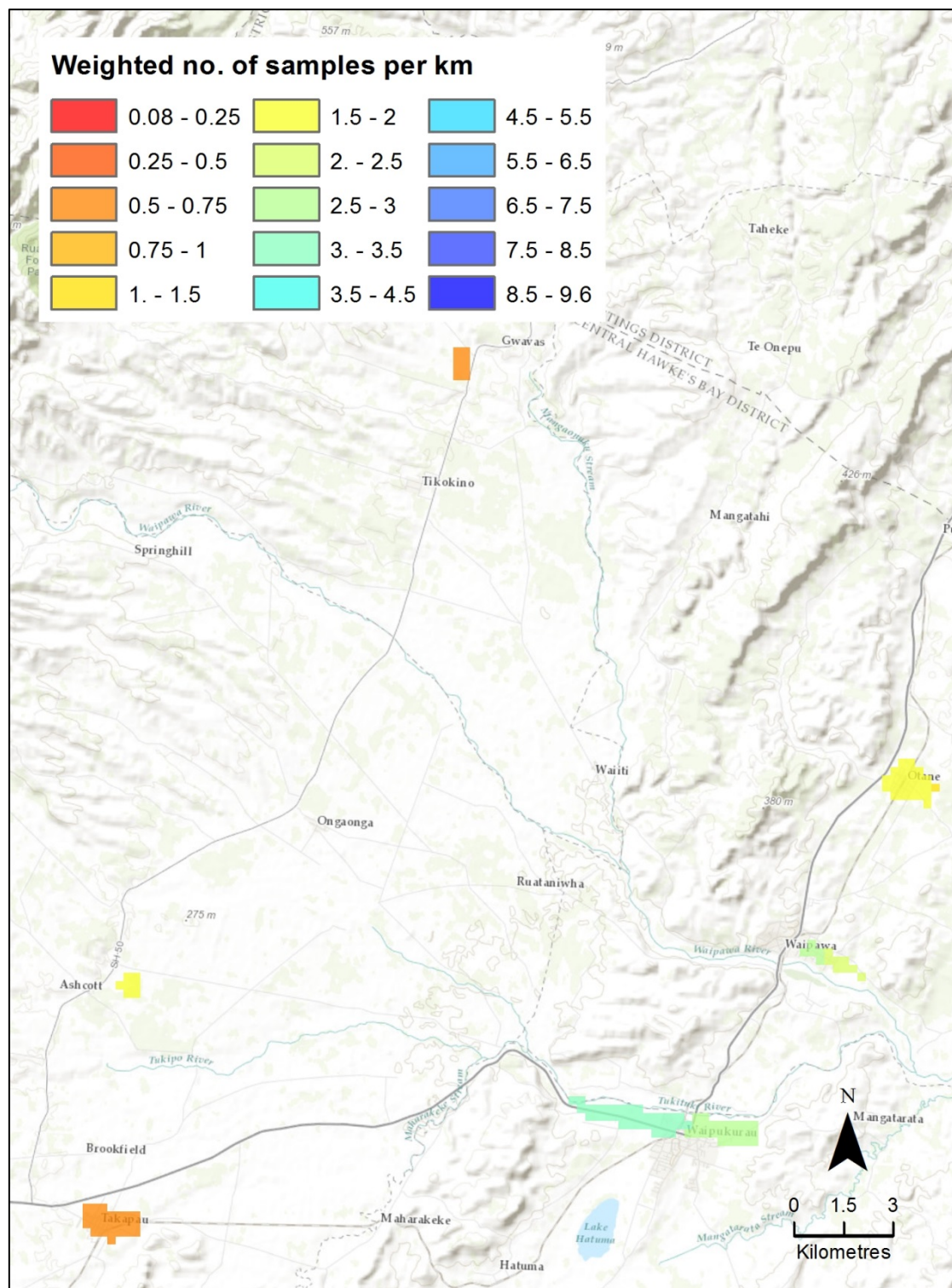


Figure A6.11 Uncertainty map for the northern portion of Zone 3, based on data point density as described in the text.

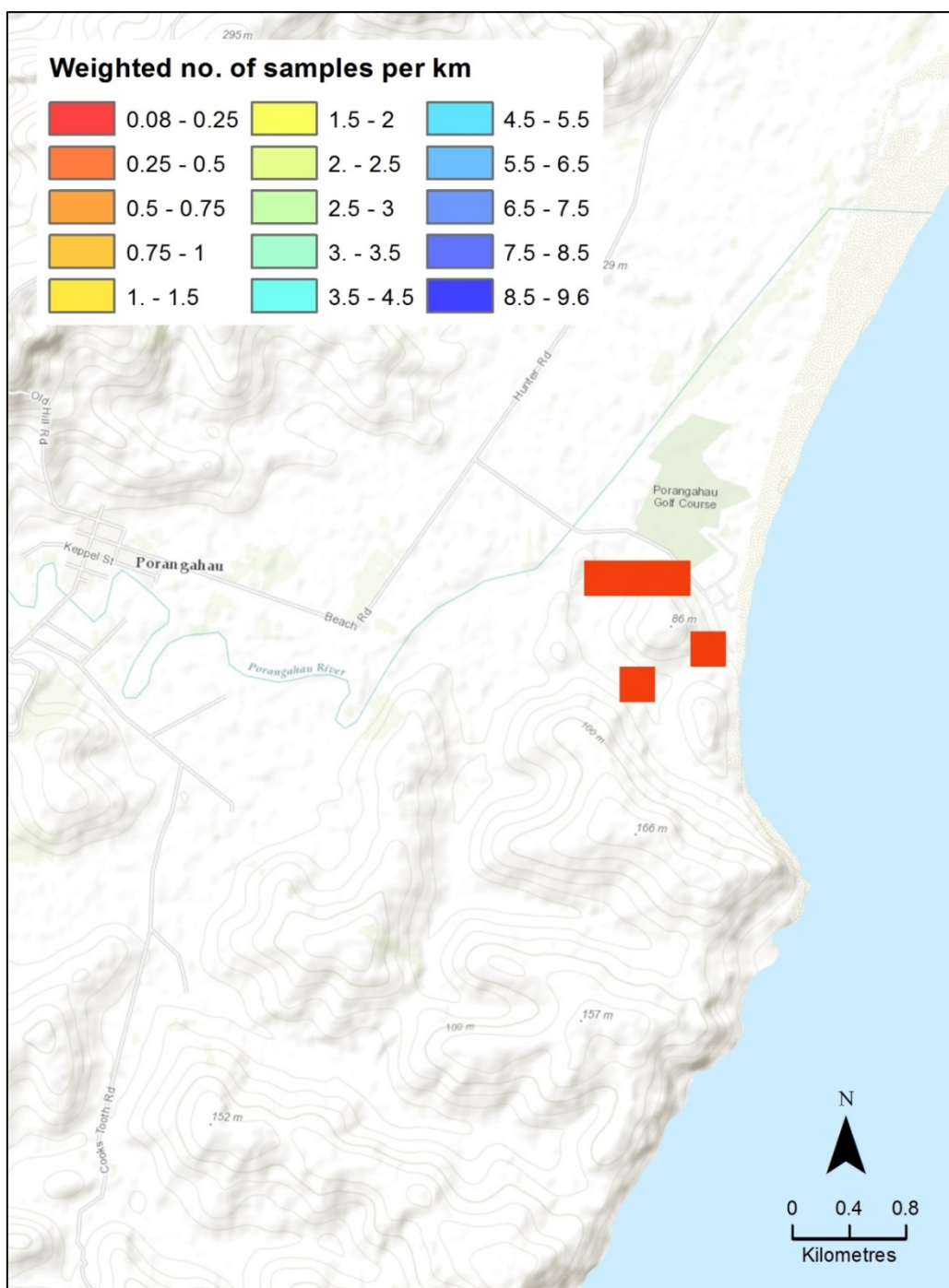


Figure A6.12 Uncertainty map for the southern portion of Zone 3, based on data point density as described in the text.

A6.4 DISCUSSION

As shown in Figure A6.2, there can be significant seasonal and yearly water level fluctuations and therefore significant deviations from the median UGS. The most appropriate quantification of risk associated with probable water saturation would therefore take into consideration not only the median UGS, but also the minimum and maximum UGS. This is currently not possible due to the scarcity of available time series data. However, these data could be used to provide statistics around the recorded fluctuations for input into Liquefaction Severity Number (LSN) calculations. The new shallow groundwater monitoring wells that were drilled by NCC for this project in early 2014 provide an example of how the uncertainty of the UGS can be reduced in the future in areas of high importance. These have provided some immediate data for the UGS calculation, although the largest uncertainty reduction from these will come after a number of years of monitoring. The UGS has been developed in mBGL and clipped to the project area due to the DEM inconsistency between LiDAR data and the national 8x8 m DEM. LiDAR data covering the entire area of interest would be useful for obtaining a consistent DEM that would allow for a surface to be developed in mASL.

A6.5 REFERENCES

- Cameron SG, Gusyev MA, Meilhac C, Minni G, Zemansky GM. 2011. Pseudo-transient groundwater-stream interaction model for determination of the effect of groundwater abstraction on spring-fed stream flow in the Poukawa basin, Hawke's Bay. Lower Hutt (NZ): GNS Science. 76 p. (GNS Science report 2011/07).
- Dravid PN, Brown LJ. 1997. Heretaunga Plains Groundwater Study, Volume 1: Findings, Hawke's Bay Regional Council, New Zealand, p. 254.
- Heron DW, Haubrock SN, Lukovic B, Rattenbury MS. 2012. QMAP seamless *G/S geological map data*, Geoscience Society of New Zealand Conference.
- Land Information New Zealand. 2014. Topo250 maps, <http://www.linz.govt.nz/land/maps/linz-topographic-maps/topo250-maps>, last accessed June 2014.
- van Ballegoooy S, Cox SC, Agnihotri R, Reynolds T, Thurlow C, Rutter HK, Scott DM, Begg JG, McCahon I. 2013. Median water table elevation in Christchurch and surrounding area after the 4 September 2010 Darfield Earthquake. Lower Hutt (NZ): GNS Science. 66 p. (GNS Science report; 2013/01).

A7.0 APPENDIX 7: TYPICAL LIQUEFACTION DAMAGE

LAND DAMAGE OBSERVATION CATEGORIES		
Simplified land damage categories used in Appendix A of this study	Land observation categories presented in the Liquefaction Vulnerability Report (T&T, 2013) and EQC Stage 3 Report	CRITERIA / DESCRIPTION
None to Minor	None Observed	<ul style="list-style-type: none"> • No observed cracks, undulation/deformations at the ground surface, and, • No signs of ejected liquefied material at the ground surface, and, • No apparent lateral movement.
Minor to Moderate	Minor	<ul style="list-style-type: none"> • Shaking-induced damage resulting from cyclic deformation and surface-waves causing ground surface damage. Ground surface damage likely limited to minor cracking (tension) and buckling (compression) and/or minor undulations at the ground surface, and, • No signs of ejected liquefied material at the ground surface, and, • No apparent lateral movement.
Moderate to Severe	Moderate	<ul style="list-style-type: none"> • Minor to moderate quantities of ejected liquefied material on ground surface (generally <25% of site covered with ejected material), and/or, • Small cracks from ground oscillations (<50 mm) may be present, but little to no vertical displacement across cracks, and, • No apparent lateral movement.
Moderate to Severe	Major	<ul style="list-style-type: none"> • Large quantities of ejected liquefied material on ground surface (generally >25% of site covered with ejected material), and/or, • Severe observed ground surface subsidence, and/or, • Small cracks from ground oscillations (<50 mm) may be present, but little to no vertical displacement across cracks, and, • Limited evidence of lateral movement.
Moderate to Severe	Severe	<ul style="list-style-type: none"> • Moderate to major lateral spreading (<1 m cumulative), and/or, • Large cracks extending across the ground surface, with horizontal and/or vertical displacement (>50 mm, but generally <200 mm), and, • Ejection of liquefied material at the ground surface may also be observed.
Moderate to Severe	Very Severe	<ul style="list-style-type: none"> • Extensive lateral spreading (≥ 1 m cumulative), and/or, • Large open cracks extending through the ground surface, with very severe horizontal and/or vertical displacements (≥ 200 mm), and, • Ejection of liquefied material at the ground surface may also be observed.

1.3

Typical photographs of none to minor land damage



Flat lawn



Slightly undulating lawn and driveway

None to minor land damage



Undamaged asphalt driveway



Aerial shot of Broomfield area showing no liquefaction ejecta on the roads or Broomfield Common

None to minor land damage



Undulating lawn



View of Centaurus Road with little damage

Typical photographs of minor to moderate land damage



Liquefaction ejecta in piles on road



Aerial photo of liquefaction ejecta at Cashmere High School

Minor to moderate land damage



Isolated area of liquefaction ejecta



Liquefaction ejecta in many places on lawn

Minor to moderate land damage



Foundation and brickwork damage



Liquefaction ejecta, dwelling tilting

Typical photographs of moderate to severe land damage



Aerial photo showing liquefaction ejecta on Seabreeze Close



Foundation damage

Moderate to severe land damage



Liquefaction ejecta piles along Androssan Street



Outside of dwelling showing level liquefaction ejecta reached on brickwork and windows

Moderate to severe land damage



Large amounts of liquefaction ejecta and tilting dwelling



Foundation damage, tilting dwelling